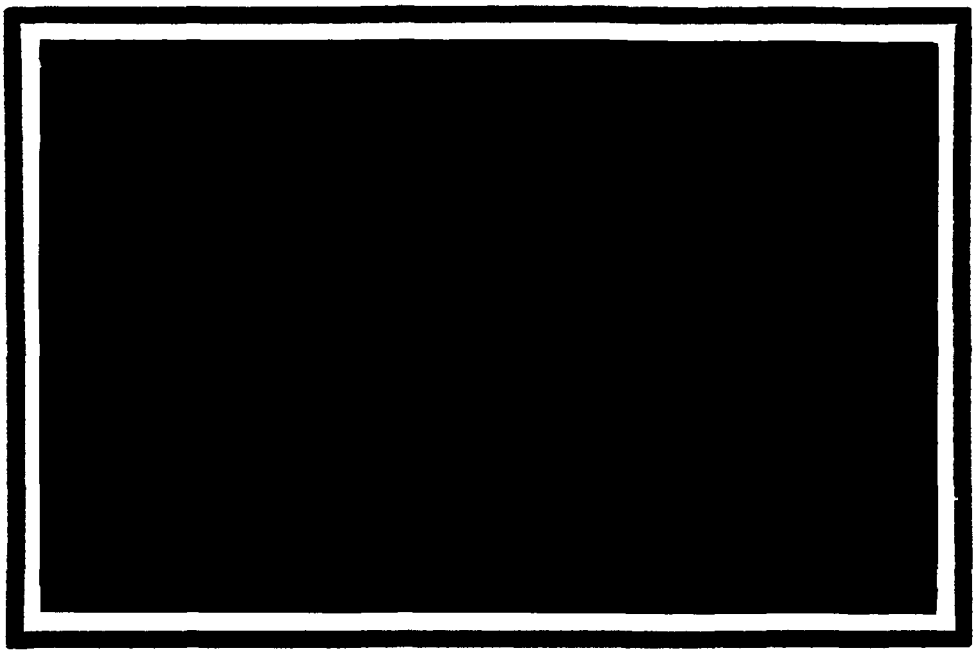

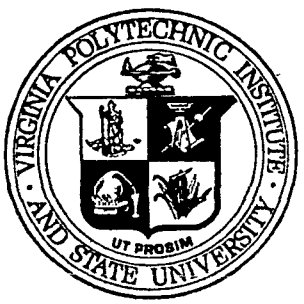

Virginia Polytechnic Institute
and State University
Department of Aerospace Engineering
Blacksburg, Virginia 24061

NASA CR-112292
March 1973

TURBULENT MIXING OF MULTIPLE, CO-AXIAL HELIUM JETS IN A SUPERSONIC AIR STREAM

A. K. Lorber and J. A. Schetz

Prepared Under Contract No. NAS1-10233
Aerospace Engineering Department
Virginia Polytechnic Institute and State University
Blacksburg, Virginia 24061

for

NATIONAL AERONAUTICS AND SPACE ADMINISTRATION

Page Intentionally Left Blank

TABLE OF CONTENTS

SUMMARY

An experimental study of a strut-mounted, five-port, coaxial gaseous fuel injector assembly in a Mach 4 air stream with P_o = 145 psia and T_o = 546^{o}R was conducted. Helium was used as the injectant, and the interjet spacing was the main parameter varied. The principal data are in the form of helium concentration profiles at six axial stations and pitot pressure profiles at two axial stations. Schlieren photographs are also presented. The slight sensitivity of the mixing rate to decreased interjet spacing was determined in the range $3.5 \leq S/D \leq 5.0$.

NOMENCLATURE

D Jet diameter

M Mach number

P_c Cone-static pressure

P_T Pitot pressure

S Centerline to centerline spacing

S/D Non-dimensional jet spacing

x axial coordinate

INTRODUCTION

Turbulent mixing of co-axial jets has been the subject of considerable study throughout this century. Ref. (1) presents a comprehensive summary of work prior to 1960. Since all turbulent "analyses" are based heavily upon empirical information, progress has been paced by the availability of experimental studies pertinent to the problem under consideration. Ref. (2) contains a tabulation of the experimental studies published up to 1969. The recent NASA workshop on Free Turbulent Shear Flows, Ref. (3) provides a ready assessment of the state-of-the-art as of the current year.

Despite the large body of information described in the references cited above, there are many practical configurations that have received little or no study. Several of these cases have been generated by the serious consideration of the SCRAM jet propulsion system. Currently available information demonstrates that the lateral spreading rate of gaseous fuels injected co-axial with the main air stream is too slow to achieve adequate mixing in a reasonable length combustor using isolated injectors. Thus, it appears attractive to consider strut-mounted, multiple injector units. This raises the important question of whether co-axial jets in close lateral proximity will result in enhanced or decreased mixing rates in comparison with the isolated, single jet case.

This report describes the results of an experimental study of two, five-port injector assemblies in a Mach 4 air stream with helium as the injectant. The major parameter varied was the centerline to centerline jet spacing, and the principal data consist of helium concentration distributions. Schlieren pictures and pitot pressure distribution were also obtained.

In the first section of this report, a complete description of the equipment and test methods employed in the research is given. Then, the experimental results are presented and discussed.

APPARATUS

A. Wind Tunnel Facilities

Tests were conducted in the 9" x 9" supersonic wind tunnel in the Gas Dynamics Lab at V.P.I. & S.U. This facility is of an intermittent, blow-down type with interchangeable contoured nozzles. A complete description of the tunnel is given in Appendix A. The Mach 4.016 nozzle was used for this experimental effort. The average starting tunnel total pressure and total temperature were 145 psia and 546^{o}R, respectively. During the tests there was a slow linear decrease in both total pressure and total temperature. In order to account for these variations, all recorded pressures and temperatures were nondimensionalized by their corresponding stagnation conditions at the time the measurements were taken. Test runs were approximately 8 seconds in duration.

B. Injection Model

Two, separate five-port injectors were constructed and tested. They were identical except for the jet centerline to centerline spacing which was 1.00 inches for injector Mod. A and 0.70 inches for Mod. B. The detailed layout for Mod. A is shown in Fig. 1 and photographs are given in Fig. 2. The models were constructed of steel with the individual injection tubes (0.250 inch O.D. x 0.196 inch I.D.) brazed to the main strut assembly. All junctions were filleted with aluminum-filled Devcon paste to produce a relatively clean aerodynamic configuration. The final configuration was determined by Schlieren observation of various arrangements of the Mod. A injector.

The struts in each model were left as clear as possible internally, and the flow from the ports on the "wings" was initially substantially lower (approx. 30%) than those on the main strut. In order to balance the mass flow from each port, thin walled sleeves with an O.D. equal to the I.D. of the tubes were inserted into the ports on the main strut. For Mod. A, tubes of 0.020", 0.010" and 0.010" wall thickness were permanently inserted in the top, center and bottom ports, respectively. The resulting pitot-pressure distributions are shown in Fig. 3a where the close agreement in mass flow per port is apparent. For Mod. B, tube of 0.020", 0.020" and 0.020" wall thickness were used to produce the results shown in Fig. 3b. The average flow rate from each port on both models was 0.37#/min. This flow rate was chosen to produce a minimum of wave disturbance in the jet at the exit.

C. Injectant Supply System

The injectant supply system is shown schematically and photographically in Figs. 4a and b. The basic elements in the system are: 1) the nine-bottle manifold for storage, 2) a ball valve, 3) a dome-regulator in parallel with a globe valve, 4) a mass flow measuring station and 5) copper tubing connectors to the top and bottom of the main strut on the fuel injector. Flow from the nine-bottle manifold was initiated by the hand operated ball valve. Flow control was achieved by a dome regulator in parallel with a globe valve which was pre-set before a run. The flow rate was determined with an ASME orifice flow meter[4]. The orifice size was 0.600 inches diameter inside a 1.357 inch inside diameter pipe. The flow rate was calculated using standard procedures with the pressure P_1 and P_2. The total flow rate for each model was 1.85#/min.

D. Pressure and Gas Analysis Instrumentation

Pressure and helium concentration distributions were obtained to define the flow field. With the rake shown in Fig. 5, pitot pressure and gas sampling surveys were taken at several axial stations. The individual tubes on the rake were 0.030" O.D. and 0.016" I.D. The pitot tubes were assigned numbers for identification as indicated in Fig. 4, and the distances between the pitot tubes are listed in Table I. Not all of the probes were used to collect samples. Sample and probe numbers are correlated in Table II. Vertical ports 7 and 11 and lateral ports 8 and 10 were located symmetrically about port 9 so that the rake could be centered in the jet by matching concentrations. Another feature of the rake was the 10^{o} half angle brass cone static probe. The base of the cone was 0.062 inches, and the tip was precision ground to a sharp point. At 0.11 inches from the tip of the cone, there were four 0.013 inch ports drilled perpendicular to the surface and 90^{o} apart. The recorded pressure was the average of these four ports. This probe was located at the mirror image of port 1, so that the Mach number variations could be determined easily if the static pressure change across the mixing region were assumed small.

Two key devices were used in positioning the rake for taking the surveys. A steel strut with a 14^{o} wedge leading edge was used to hold the rake. The strut was 20.5 inches high with a base 6 inches by 3 inches by 0.5 inches. There was a .625 inch diameter hole 20 inches above the base for the rake, and the base of the strut was bolted to a milling machine bed. This device was used for both lateral and vertical positioning of the rake. The micrometer associated with vertical location of the rake was graduated in .001 of an inch. The micrometer that indicated lateral position was marked in .001 of an inch.

The pressure leads from the rake, including the static pressure leads, were connected to a Model 48J9-1021 Scani-valve. The pressure field could be scanned once per test or nearly so as determined by scan rate and tunnel run time. A time step of .5 seconds was chosen so that the static pressure could also be read from the Scani-valve. Another advantage of this device is that it requires only one transducer. In these experiments a Statham PM 131 TC $\pm$ 50-350 SER 51926 $\pm$ 50 P51D transducer was found to be adequate. All pressures were read out on Hewlett-Packard strip chart recorders with a maximum deflection of 10 inches, accuracy of 0.1% of full scale setting, and response time of 0.25 sec.

When gas sampling tests were being run, the leads form the rake were run to a 14 bottle, solenoid-valved collection cart shown in Fig. 6. The sampling lines were continuously purged by a vacuum pump, and then the flow was diverted into the collection cart for about 3 seconds. The total cart and each sample bottle were leak-checked by pressurization with pure helium for 48 hours. Spot checks at sub-atmospheric pressure were also run.

Analysis of the gas samples was obtained using a Perkin-Elmer Model 900 Gas Chromatograph with a Carle, 0.1 ml Sample Loop, Insertion Valve. Calibration and data reduction procedures are described in Appendix B.

E. Optical Methods

Schlieren photographs were taken in order to optically visualize the flow field. A 12 inch Schlieren apparatus with two parabolic mirrors, each having a focal length of 80 inches, and an air cooled high intensity mercury-arc PEK light source was used with a 1 millisecond exposure. In order to depict the turbulent character of the flow field, spark Schlieren pictures were also taken. The light source was an EG&G 549 Microflash system with a 1μ sec. flash. Photographs were taken on Polaroid type 56 (ASA 3000) sheet film using a Graphlex camera.

PRESENTATION OF DATA

Schlieren photographs of the flow field with helium injection are shown in Fig. 7a and 7b for injectors Mod. A and Mod. B, respectively. The flow is from left to right, and both the disturbances produced by the strut and the mixing region from each jet are clearly visible. The shock waves produced by the strut and the small "wings" were minimized by streamlining the junctions of the injection tubes and the main strut. A relatively clean air flow was achieved in the mixing region. The Mach number in the wake immediately behind the strut and in line with the three vertical injection tubes was measured as approximately 2. This region represents the "free stream" for the mixing region in the near field.

The principal data obtained in this study are helium concentration profiles at x/D = 1, 6, 12, 23, 35 and 46 for both models. Actual Distances vs. x/D are given in Table III. Plots of the data are given in Figs. 8a-f and 9a-f. The profiles were measured with the rake shown in Fig. 5 in two positions; Position 1 had probe #9 on the jet centerline with the rake inverted from the view in Fig. 5, and Position 2 had the rake moved down such that probes #1 and #2 spanned the centerline. The data from the two positions thus overlapped and they are whown as open and closed symbols respectively on Figs. 8a-f and 9a-f.

An obvious feature of these profiles is that they do not have a simple, symmetrical bell-type shape as is commonly encountered in idealized jet problems. The sometimes double-peaked shape (see especially Fig. 9a) has been traced to the method used here for reducing the mass flow out of some ports in order to achieve a close match between all five ports on each model. Referring to Fig. 3a and b, it can be seen that the clean ports on the side "wings" of each model had a much more usual exit profile

shape than those on the main strut which had the flow reducing inserts. Indeed the profiles from the ports on the main strut had the same shape before the inserts were put in place. It should be noted that the pitot pressure plots describe a distribution across the nozzle and were taken very near the nozzle exit, specifically @ x/D = 1. At this distance the flow field was still influenced by its passage in the strut and the turn into the nozzle. There was no way to correct this situation and the sleeves were used only to modify the total area under the pressure distribution curves but could not modify the shape of the curve itself. The only way to do that would have been to use a considerably longer nozzle. (Present nozzle length was somewhat more 5D.) However, two additional checks were made to insure that the profile shapes obtained were real and not due to any possible shifting the flow in response to rake movement from Position 1 to Position 2 or vice versa. First, Schlieren photographs at x/D = 1 were carefully examined with the rake in both positions to look for any shift in the flow. None was observed, and the photographs for Mod B are included here as Fig. 11. Secondly, a special test series was run with a single probe reaching 0.5 inches ahead of the others on the rake. This probe was traversed across the flow at x/D = 1 for Mod. B, and the data obtained in this way are shown as triangles on Fig. 9a. The close agreement with the rake data is apparent. Thus, we are confident that the profile data presented represent the actual flow field faithfully. Clearly, however, some nicety of symmetry and order in the flow have been sacrificed in order to provide equal mass flow out of each port on each injector.

The asymmetry of the profiles makes direct assessment of the data difficult. For example, plots of the jet centerline concentration versus axial distance have little meaning here. However, it is instructive to

compare the maximum concentration versus axial distance for the two injectors. Overall, they are approximately equivalent. For example, the maximum concentrations measured are virtually equal at x/D = 6 and 46 and generally close at most other stations. From a practical fuel injector standpoint, the fact that the profiles at x/D = 46 are more or less equivalent means that the variation in inter-jet spacing had no important effect on the mixing rate. There is a measured merging of port to port mixing regions for Mod. B as can be seen in Figs. 9c, d, e, and f.

The pitot pressure distributions at two stations are given in Fig. 10. It appears that model A, with the wider spaced injection ports, constitutes more of a blockage to the tunnel flow than model B. This conclusion is supported also by the difference in amount of scatter which is considerably higher for model A.

DISCUSSION

An experimental study of the effects of adjacent jets on the mixing rate of a co-axial jet in a high speed air stream has been conducted. The conditions of the experiment in terms of Mach number, the ratio of injectant to freestream molecular weight and pressure were representative of the SCRAM jet combustion chamber. The results show that there is no important change in mixing rate, expressed in terms of the Helium concentration in the air stream, as the interjet spacing is reduced to the point where the mixing zones begin to interact in an axial distance corresponding to a combustion chamber length. An aerodynamically clean, stable support system was also developed.

REFERENCES

1. Abramovich, G. N., The Theory of Turbulent Jets, MIT Press, Cambridge (1963).
2. Schetz, J. A., "Unified Analysis of Turbulent Jet Mixing", NASA CR-1382 (1969).
3. Proceedings of the NASA Workshop on Free Turbulent Shear Flows, NASA SP-321, Vol. 1 Conference proceedings; Vol. 2 Summary of Data, July 1972.
4. Fluid Meters Handbook, American Society of Mechanical Engineers, New York.
5. McNair, H. M. and Bonelli, E. J., Basic Gas Chromatography, Varian Aerograph, Walnut Creek, Calif., 1969.

TABLE I

PROBE SPACING

Port Numbers	Distances (in.)
P_c-9	.524
11-9	.100
8-9	.100
10-9	.100
9-7	.050
7-6	.050
6-5	.050
5-4	.050
4-3	.75
3-2	.100
2-1	.125

TABLE II

SAMPLE NUMBERING

Probe Number	Sample Number
1	1
2	2
3	3
4	4
5	-
6	5
7	-
8	-
9	6
10	-
11	7
P_c	-

TABLE III

MEASUREMENT STATIONS

ACTUAL DISTANCE DOWNSTREAM IN INCHES*	NON-DIMENSIONAL DISTANCE x/D
0.1875	1
1.125	6
2.25	12
4.50	23
6.75	35
9.0	46

* Measured from injector's nozzle tip.

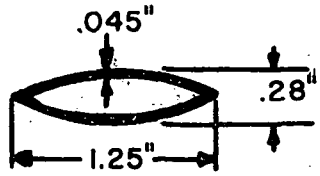

SECTION A-A

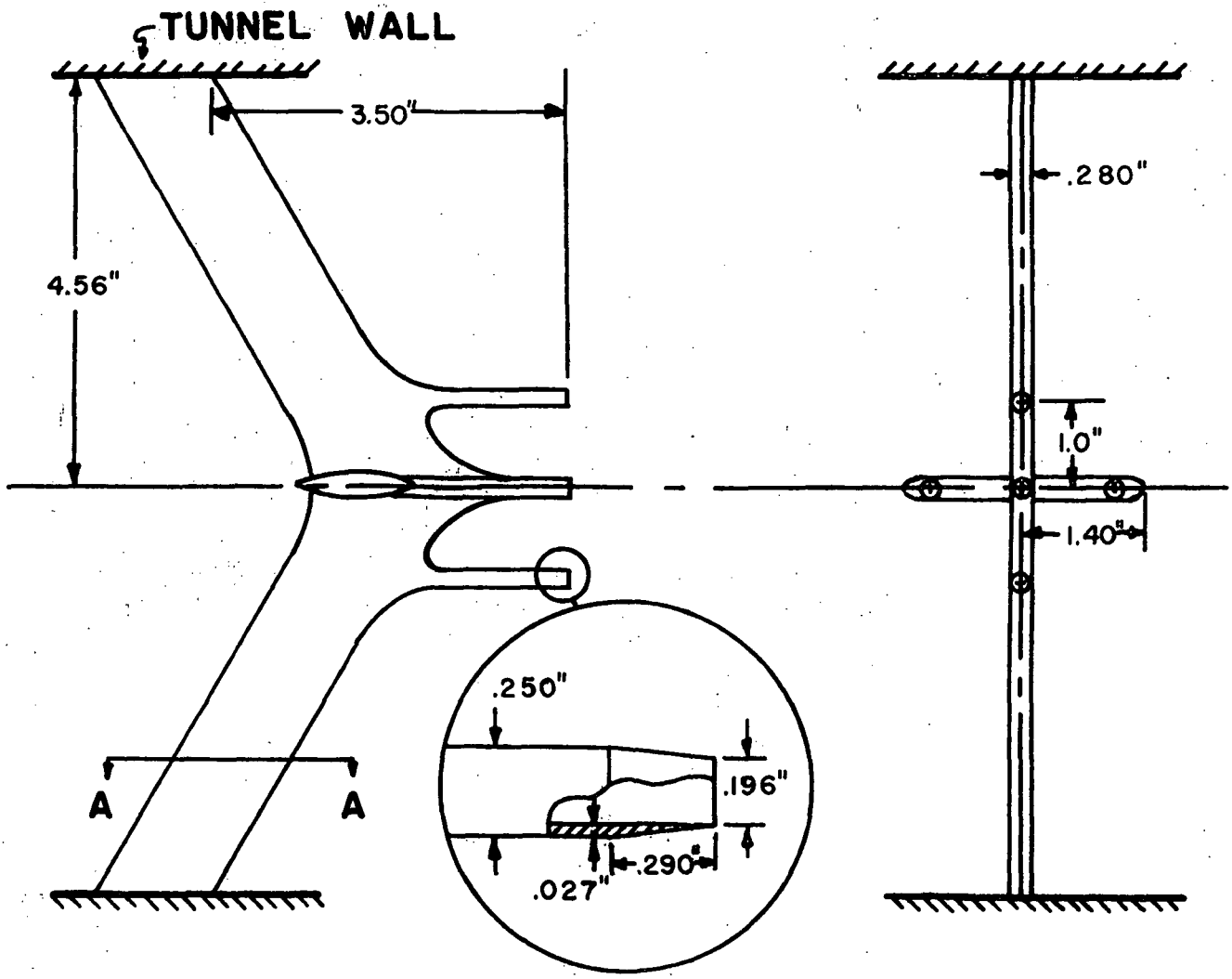

FIG. 1 DRAWING OF FIVE PORT INJECTOR (MOD. A)

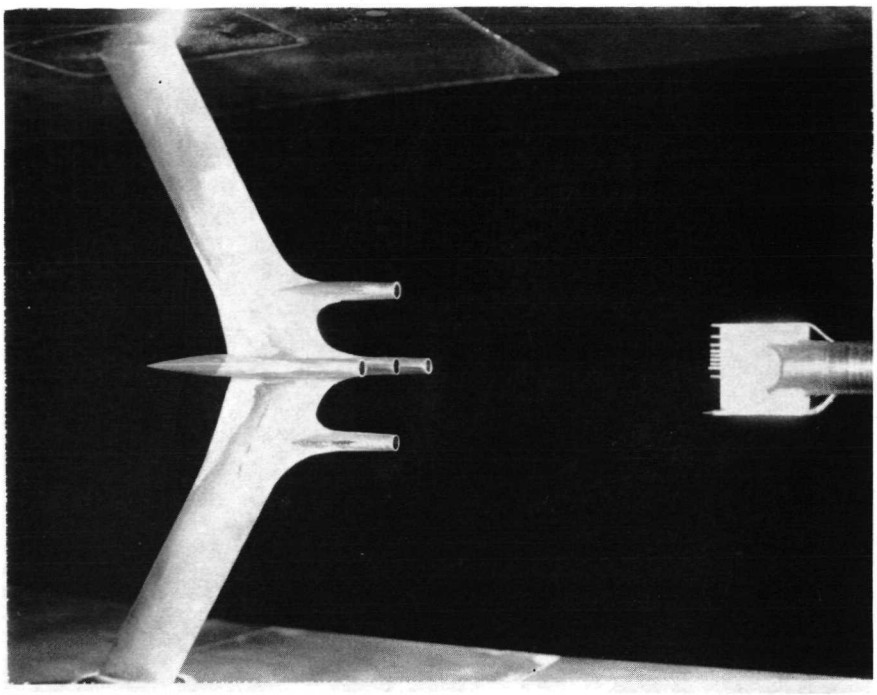

(a) Mod. A

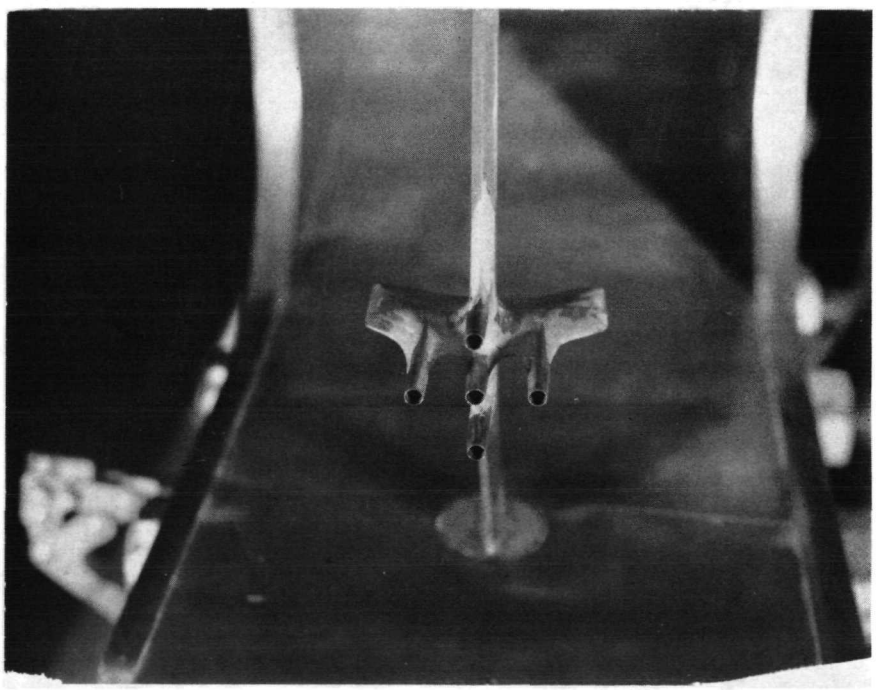

(b) Mod. B

Fig. 2 Photographs of Five Port Injectors.

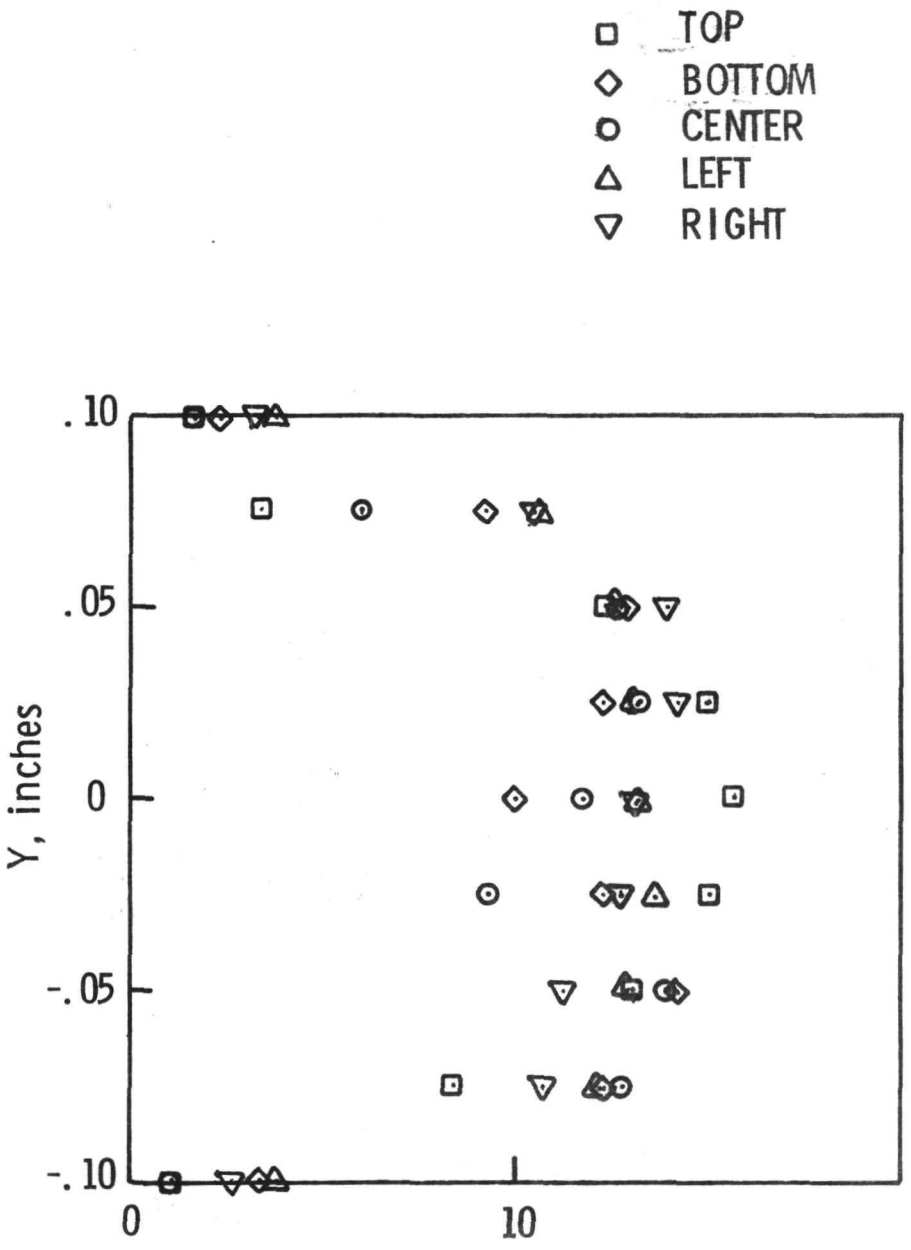

FIG. 3 PITOT-PRESSURE PROFILES AT PORT EXIT

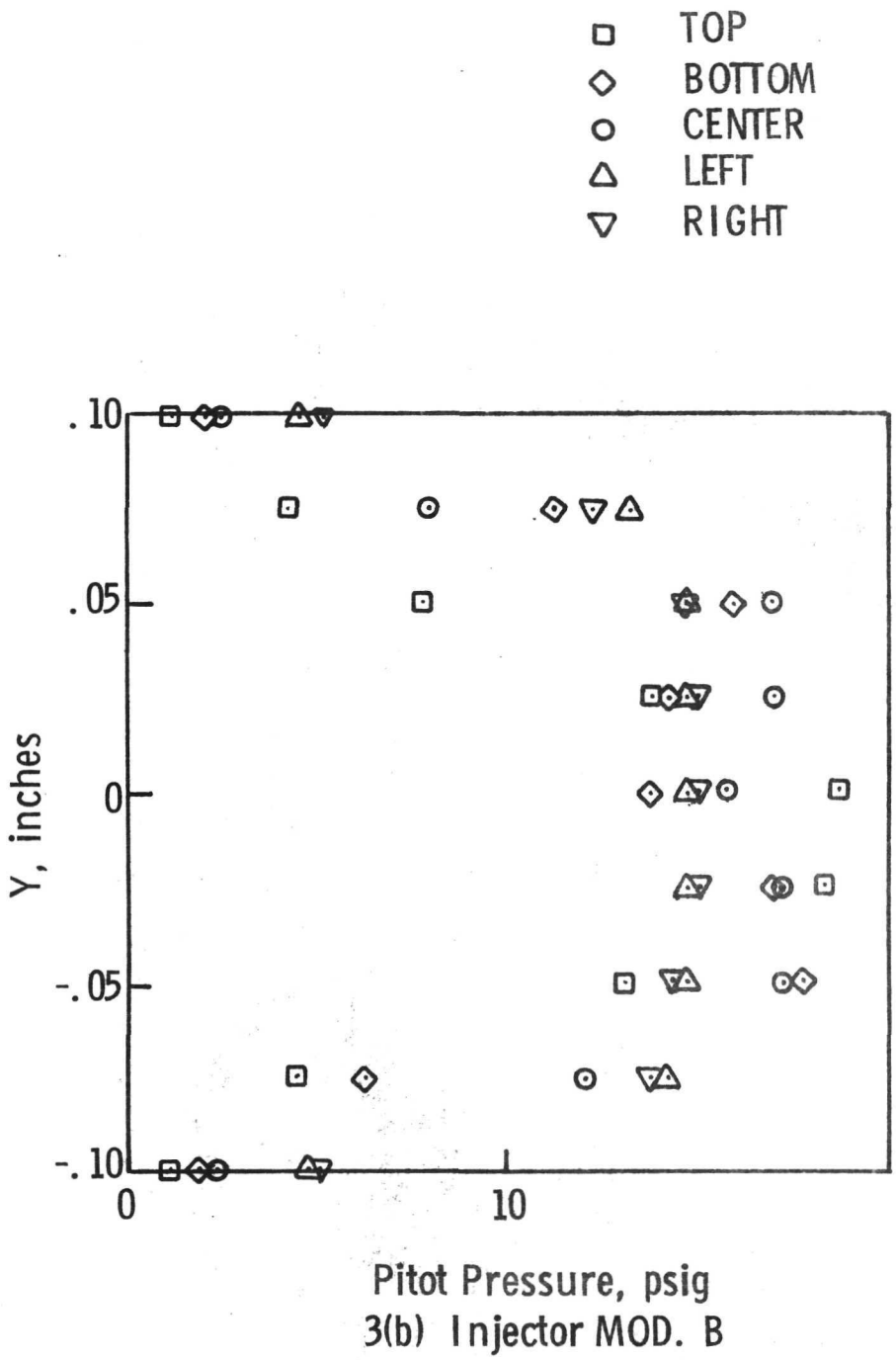

3(b) Injector MOD. B

FIG. 3 (Cont'd)

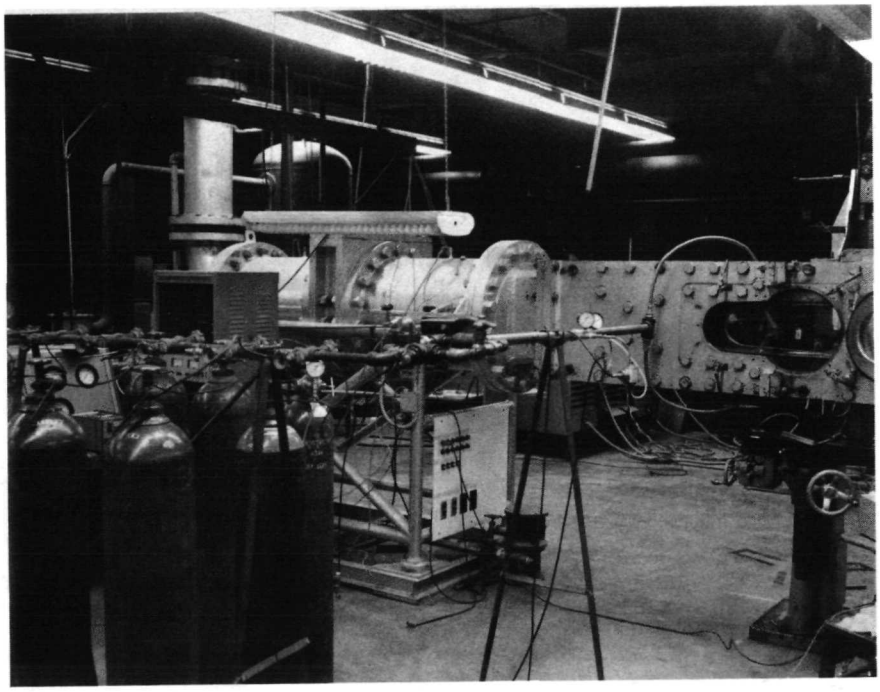

Fig. 4a Photograph of Injectant Supply System

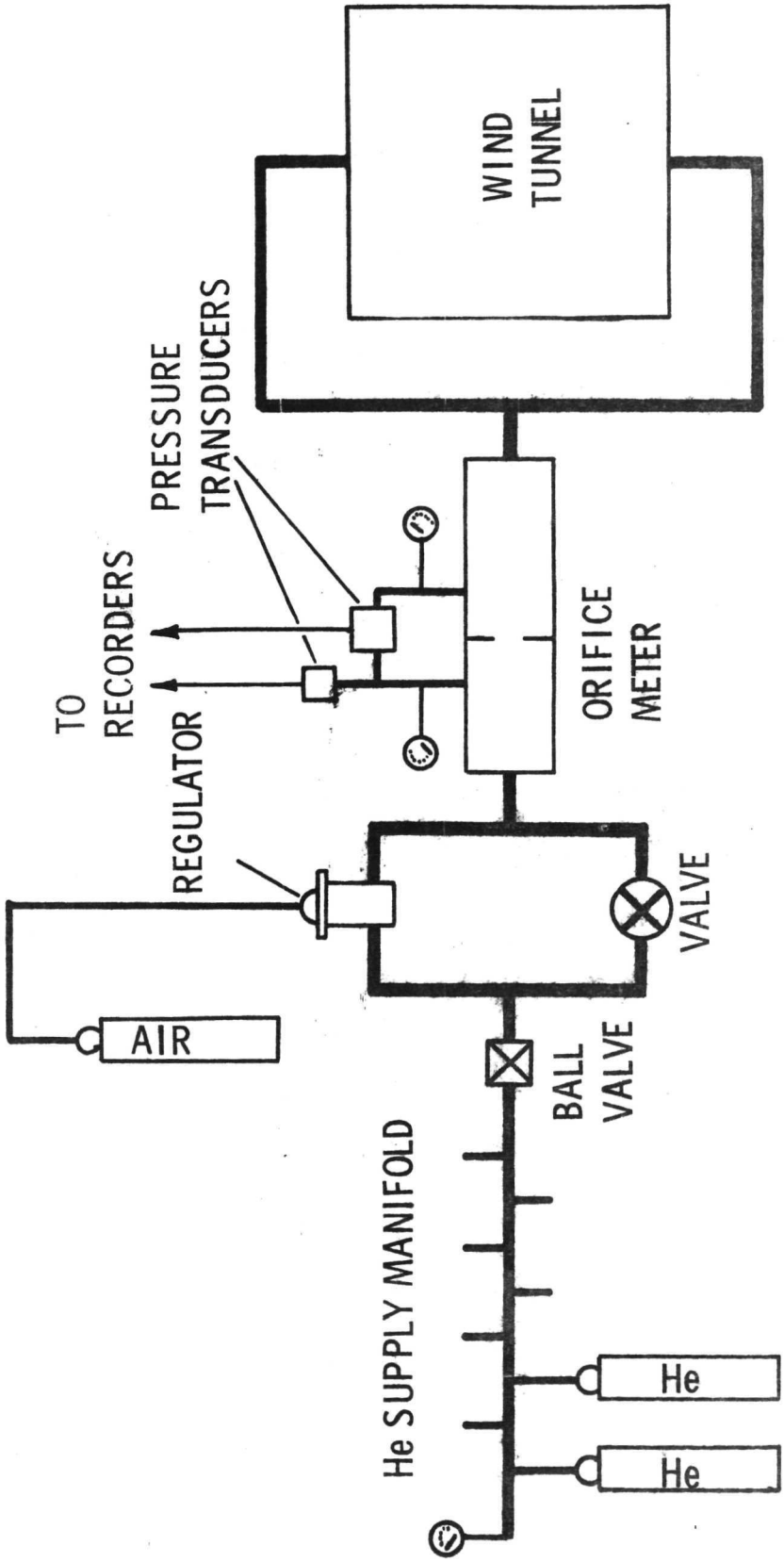

FIG. 4b SCHEMATIC DIAGRAM OF INJECTION SYSTEM

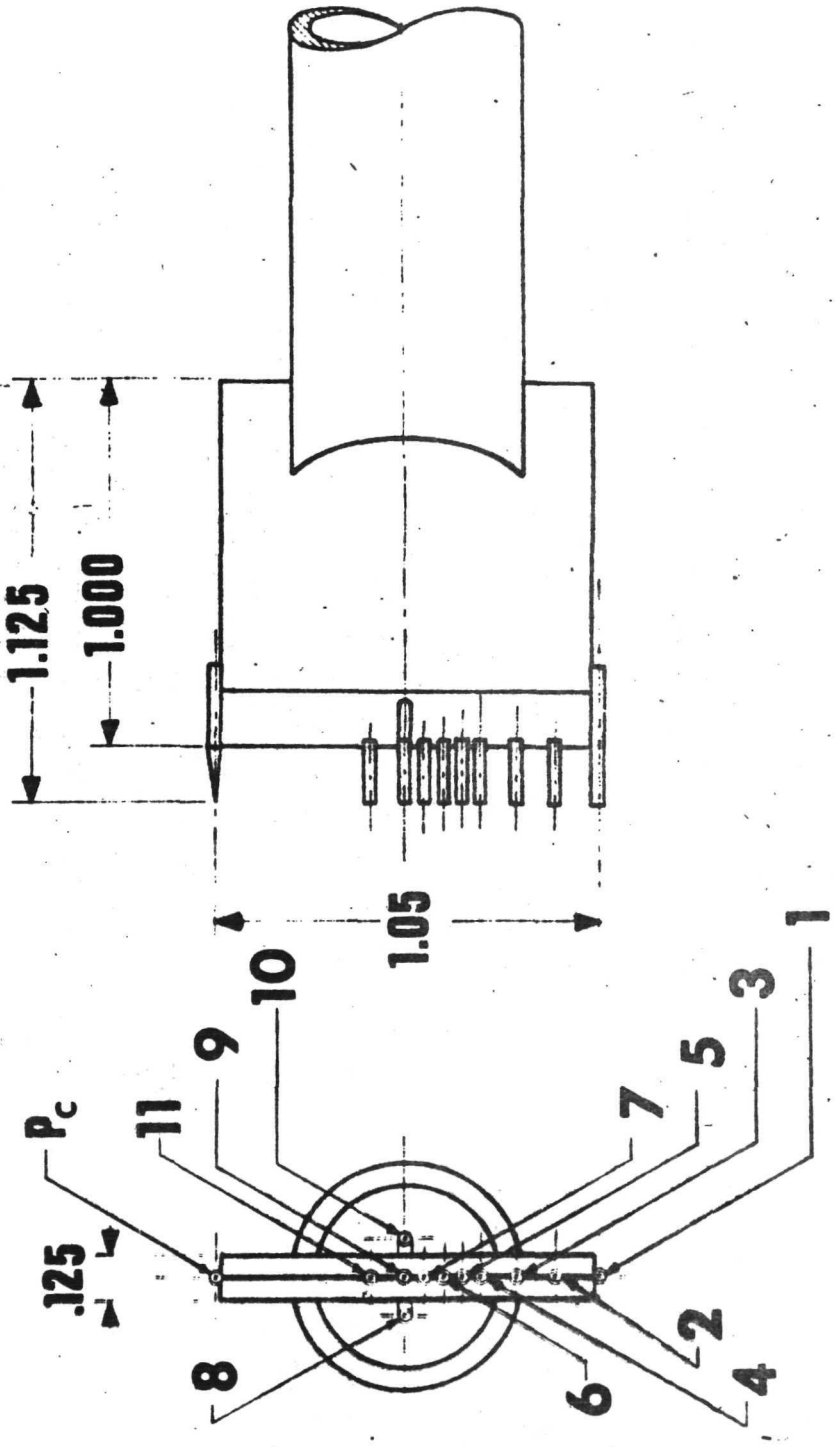

FIG. 5 RAKE DETAILS

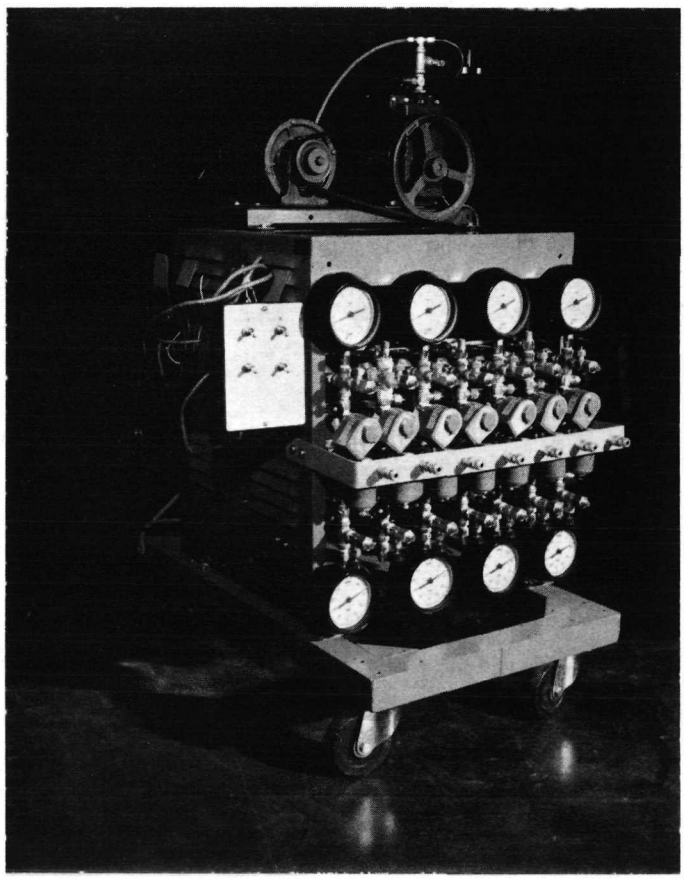

Fig. 6 Photograph of Gas Sample Collection Cart.

(a) Mod. A

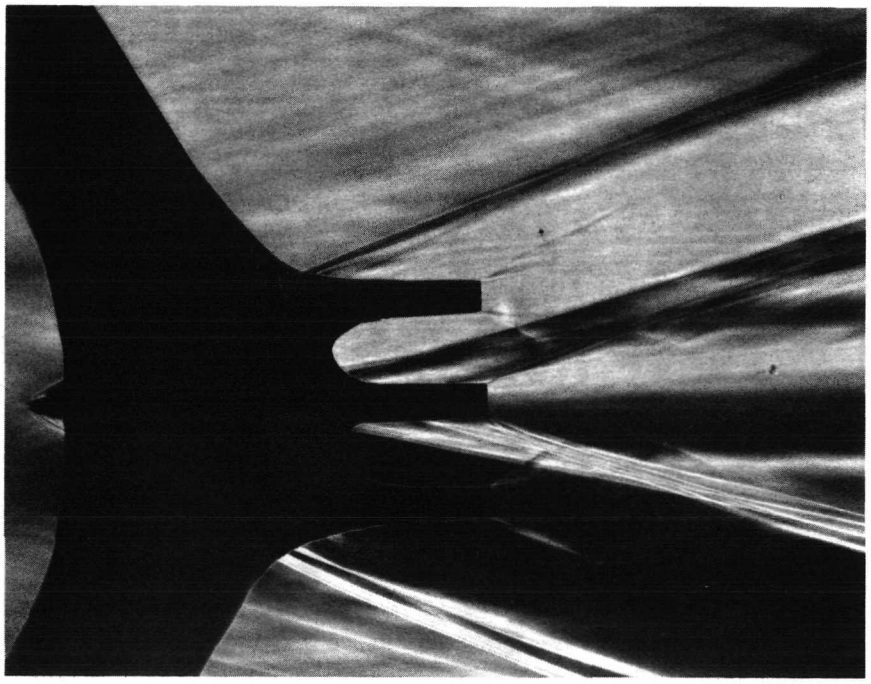

(b) Mod. B

Fig. 7 Schlieren Photographs of Flowfields with Helium Injection.

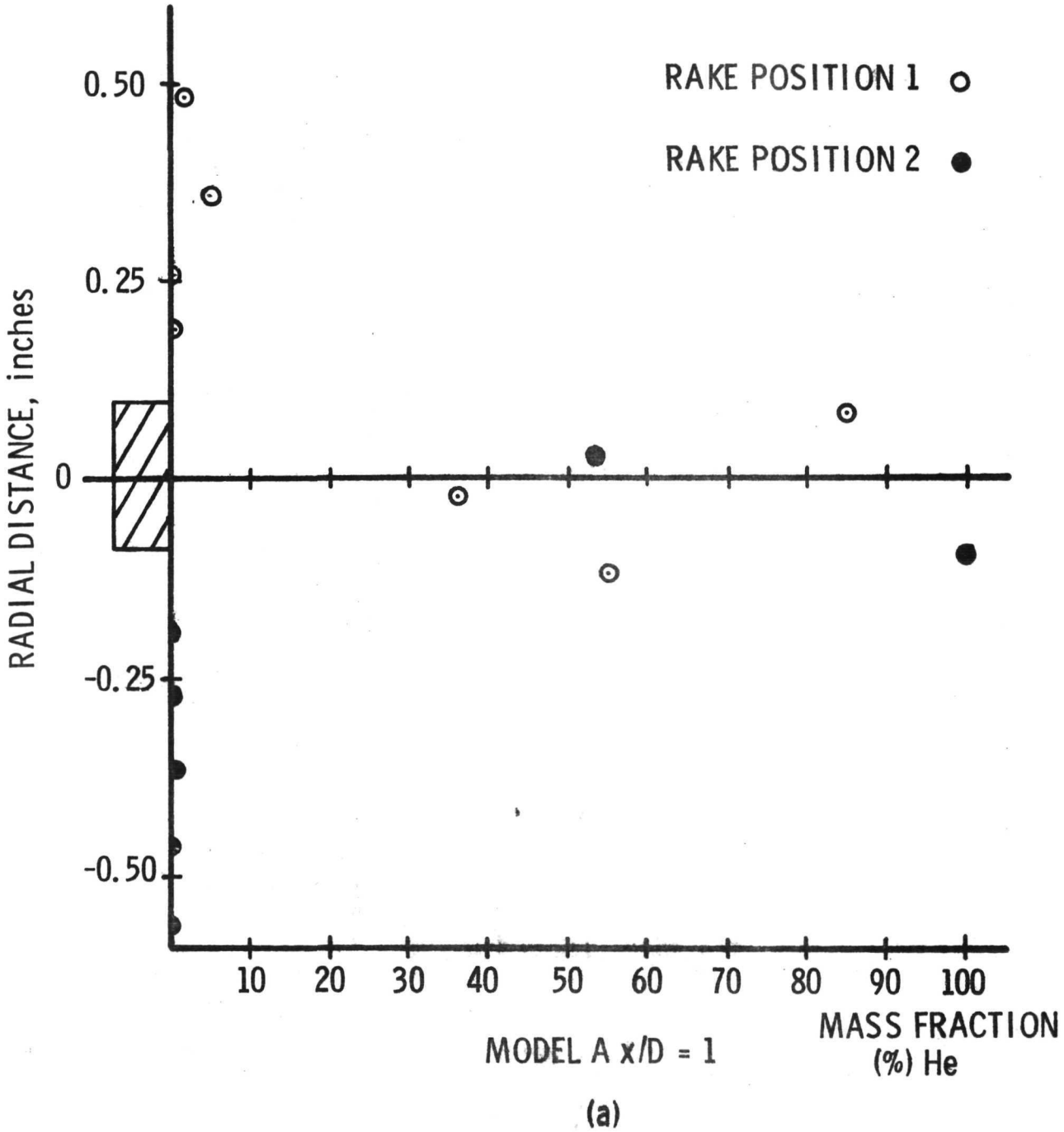

FIG. 8 HELIUM CONCENTRATION PROFILES FOR MOD. A

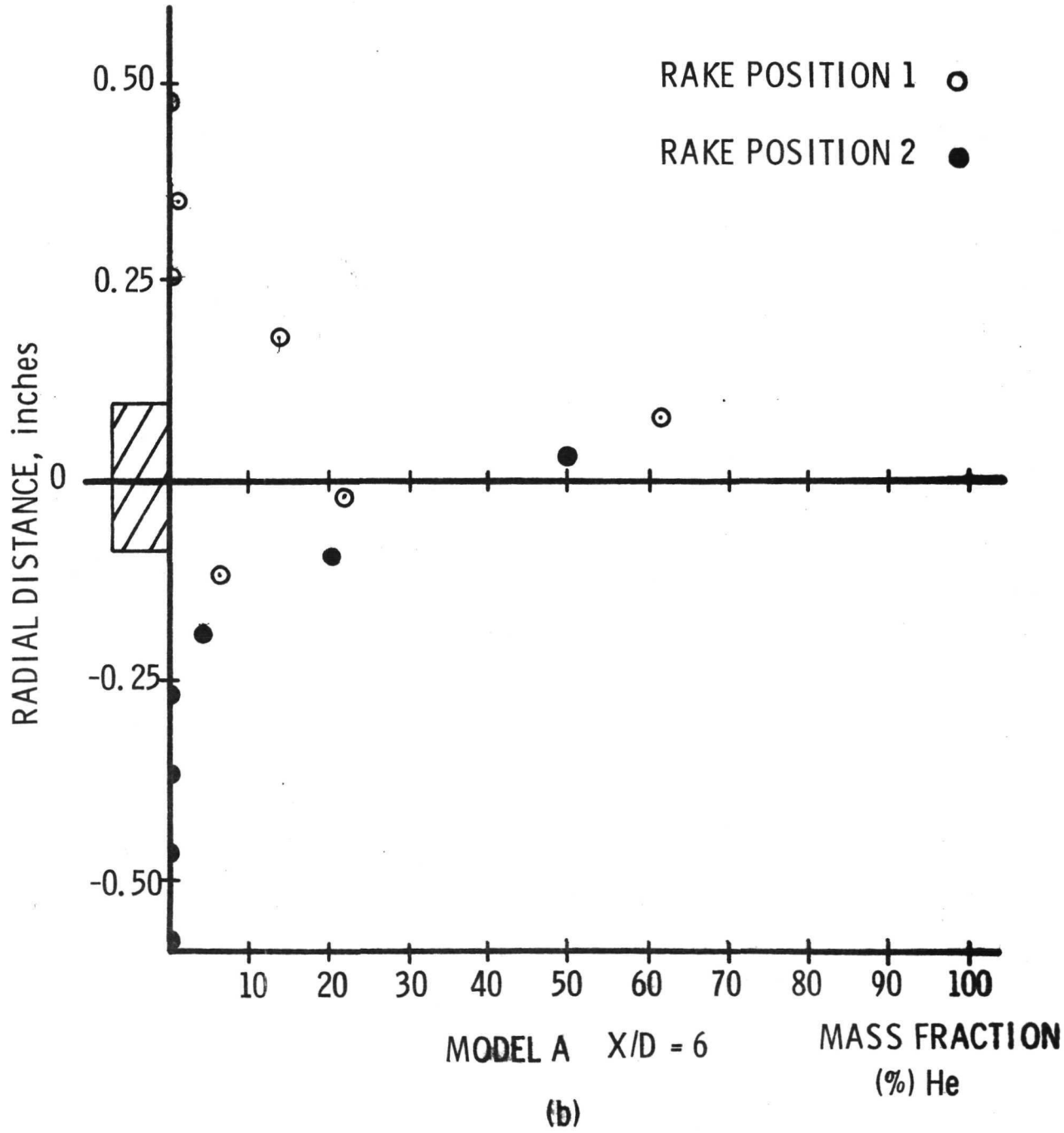
RAKE POSITION 1
RAKE POSITION 2
0.50
0.25
0
-0.25
-0.50
RADIAL DISTANCE, inches
10
20
30
40
50
60
70
80
90
100
MODEL A X/D = 6
MASS FRACTION
(%) He

(b)

FIG. 8 (Cont'd)

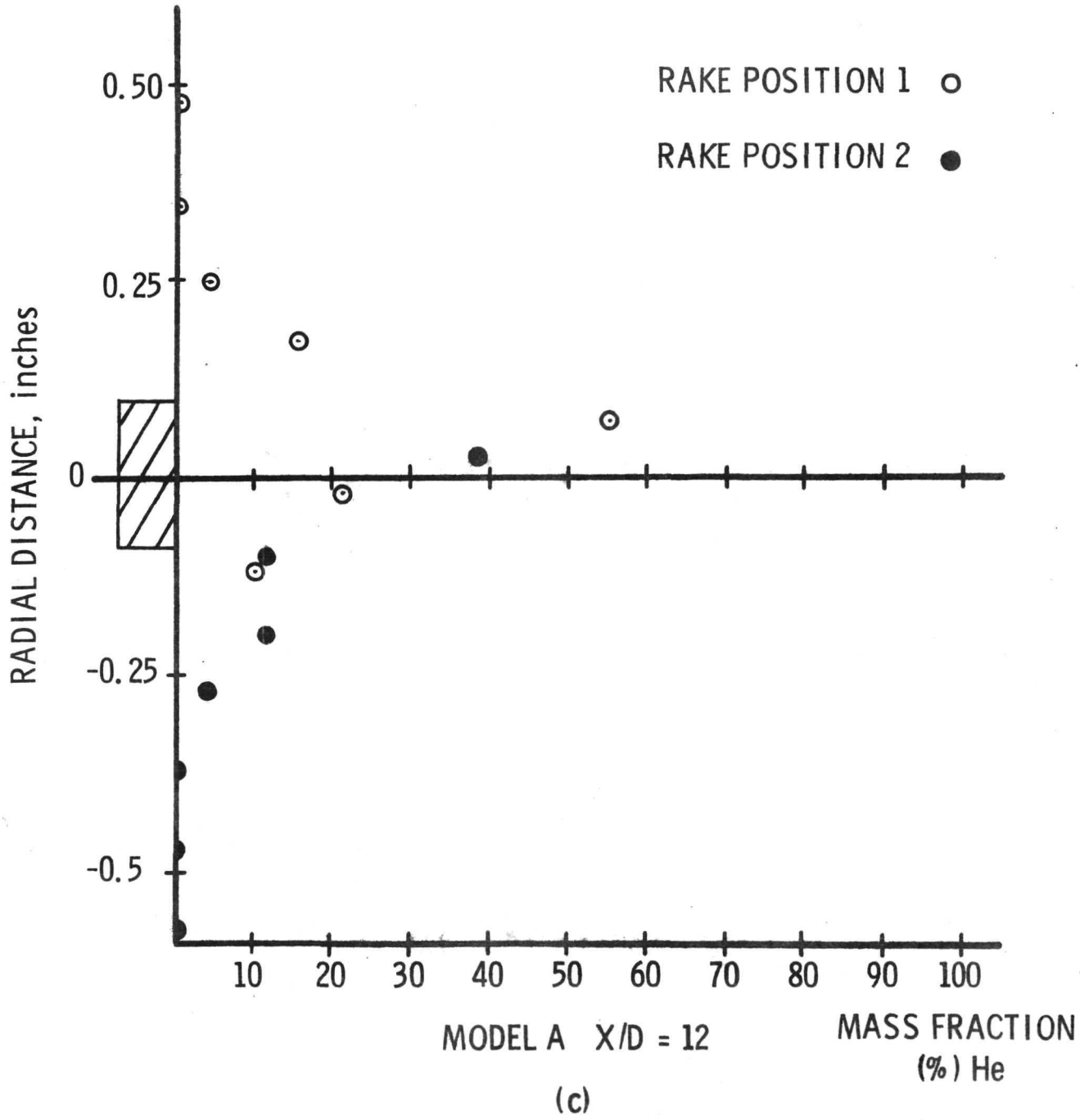
RAKE POSITION 1
RAKE POSITION 2
0.50
0.25
0
-0.25
-0.5
RADIAL DISTANCE, inches
10
20
30
40
50
60
70
80
90
100
MODEL A X/D = 12
MASS FRACTION
(%) He

(c)

FIG. 8 (Cont'd)

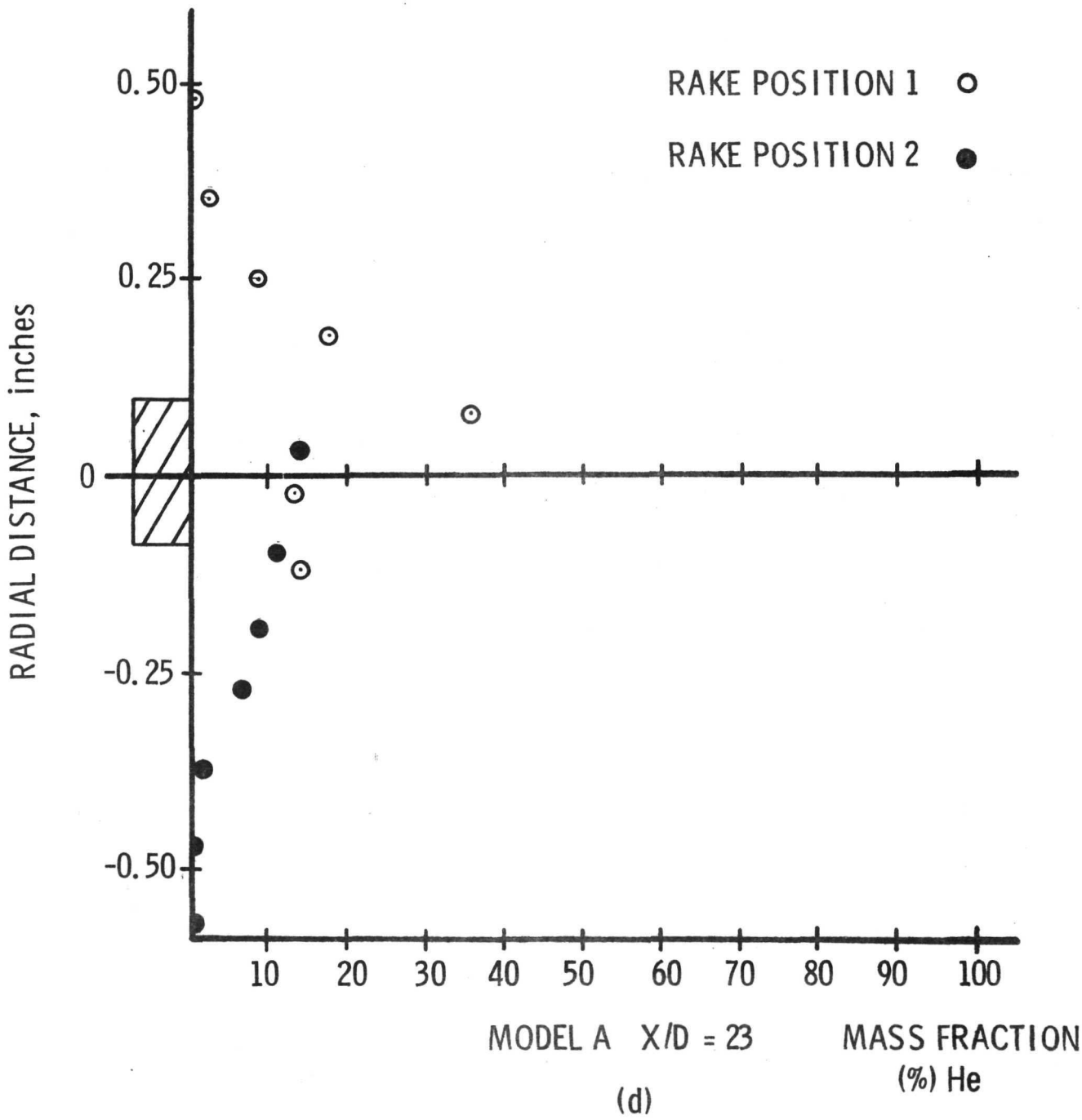
RAKE POSITION 1
RAKE POSITION 2
0.50
0.25
0
-0.25
-0.50
RADIAL DISTANCE, inches
10
20
30
40
50
60
70
80
90
100
MODEL A X/D = 23
MASS FRACTION
(%) He
(d)

FIG. 8 (Cont'd)

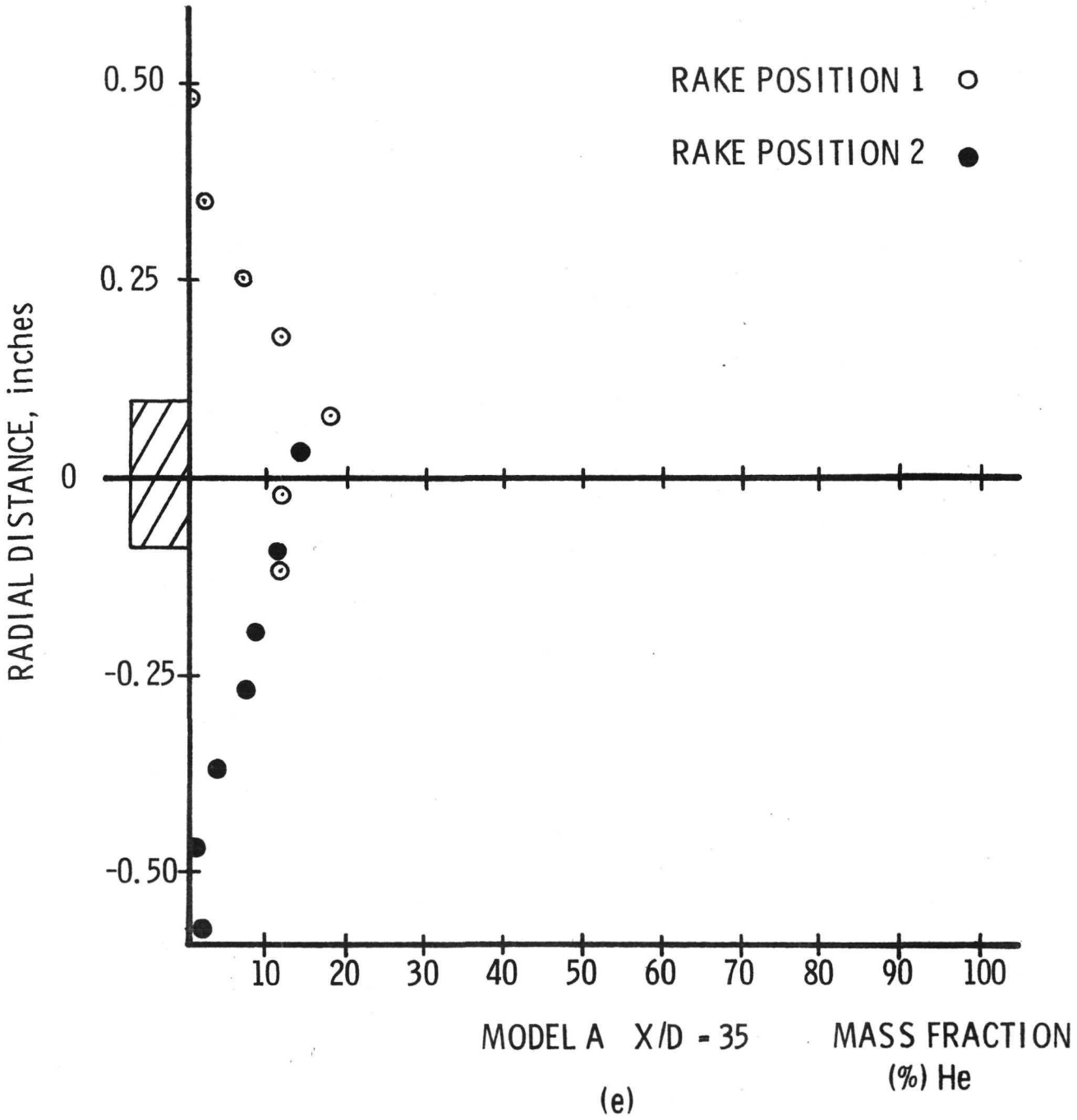
RAKE POSITION 1
RAKE POSITION 2
0.50
0.25
0
-0.25
-0.50
RADIAL DISTANCE, inches
10
20
30
40
50
60
70
80
90
100
MODEL A X/D = 35
MASS FRACTION
(%) He
(e)

FIG. 8 (Cont'd)

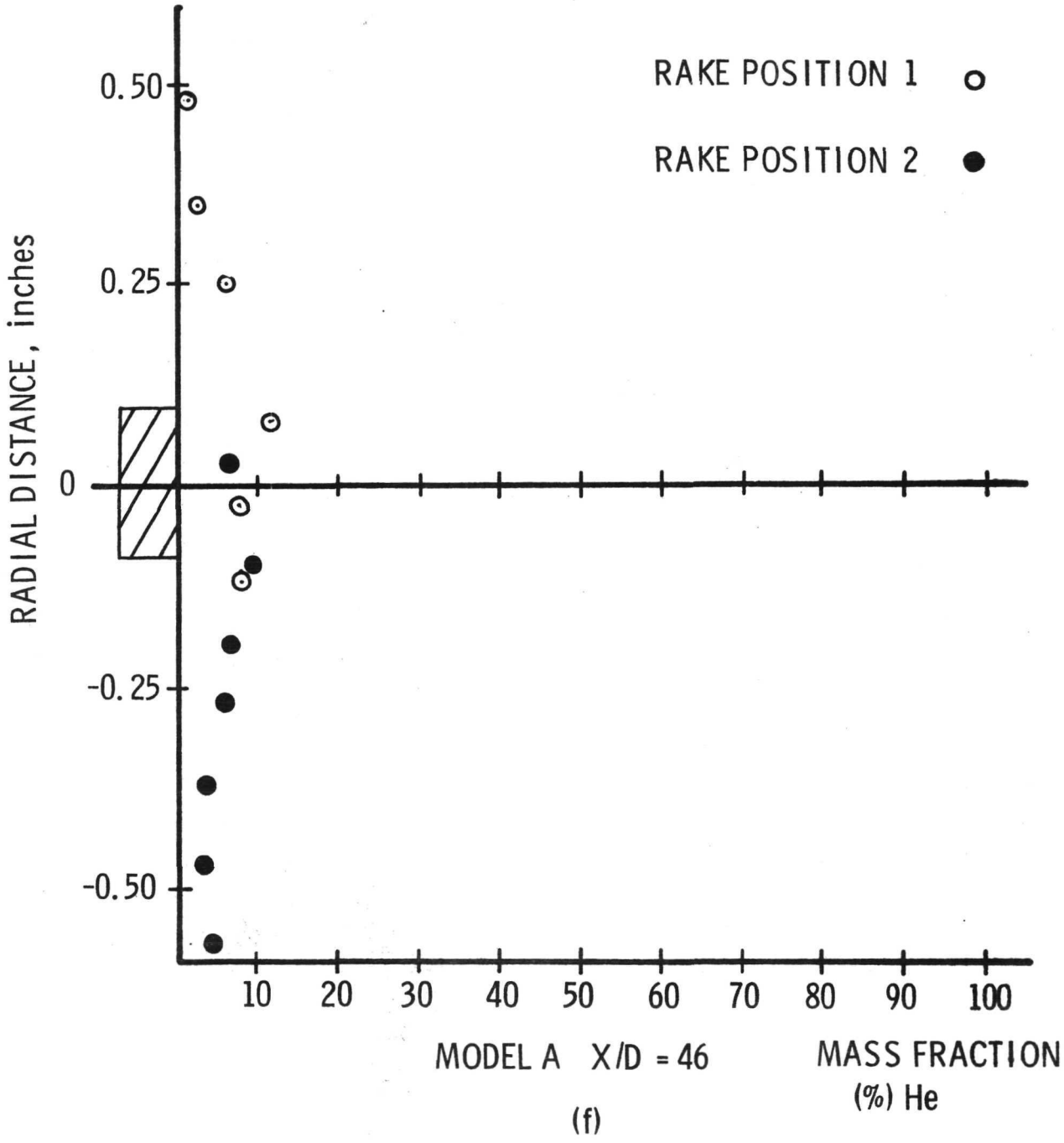
RAKE POSITION 1
RAKE POSITION 2
0.50
0.25
0
-0.25
-0.50
RADIAL DISTANCE, inches
10
20
30
40
50
60
70
80
90
100
MODEL A X/D = 46
MASS FRACTION
(%) He

(f)

FIG. 8 (Cont'd)

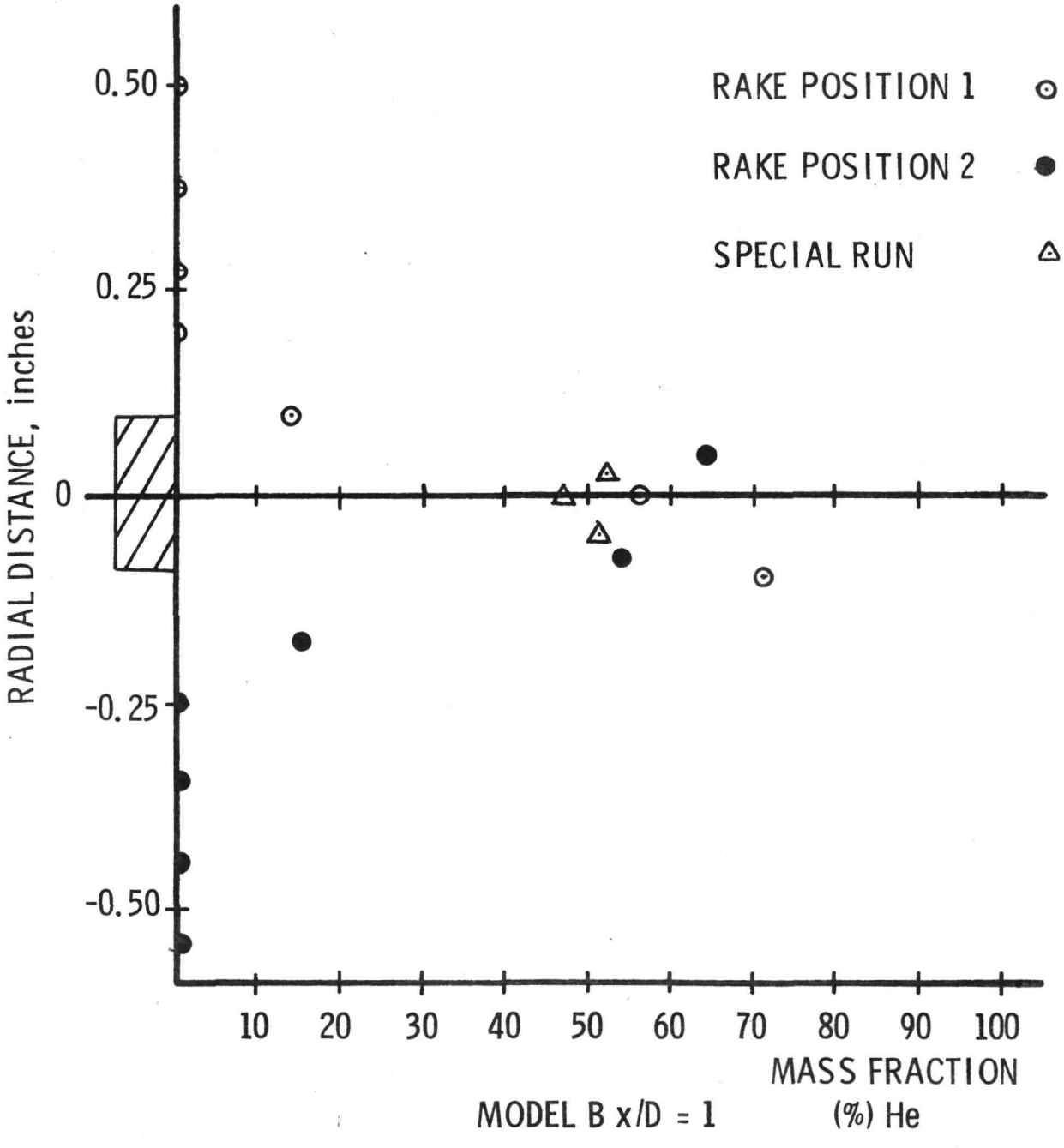

(a)

FIG. 9 HELIUM CONCENTRATION PROFILES FOR MOD. B

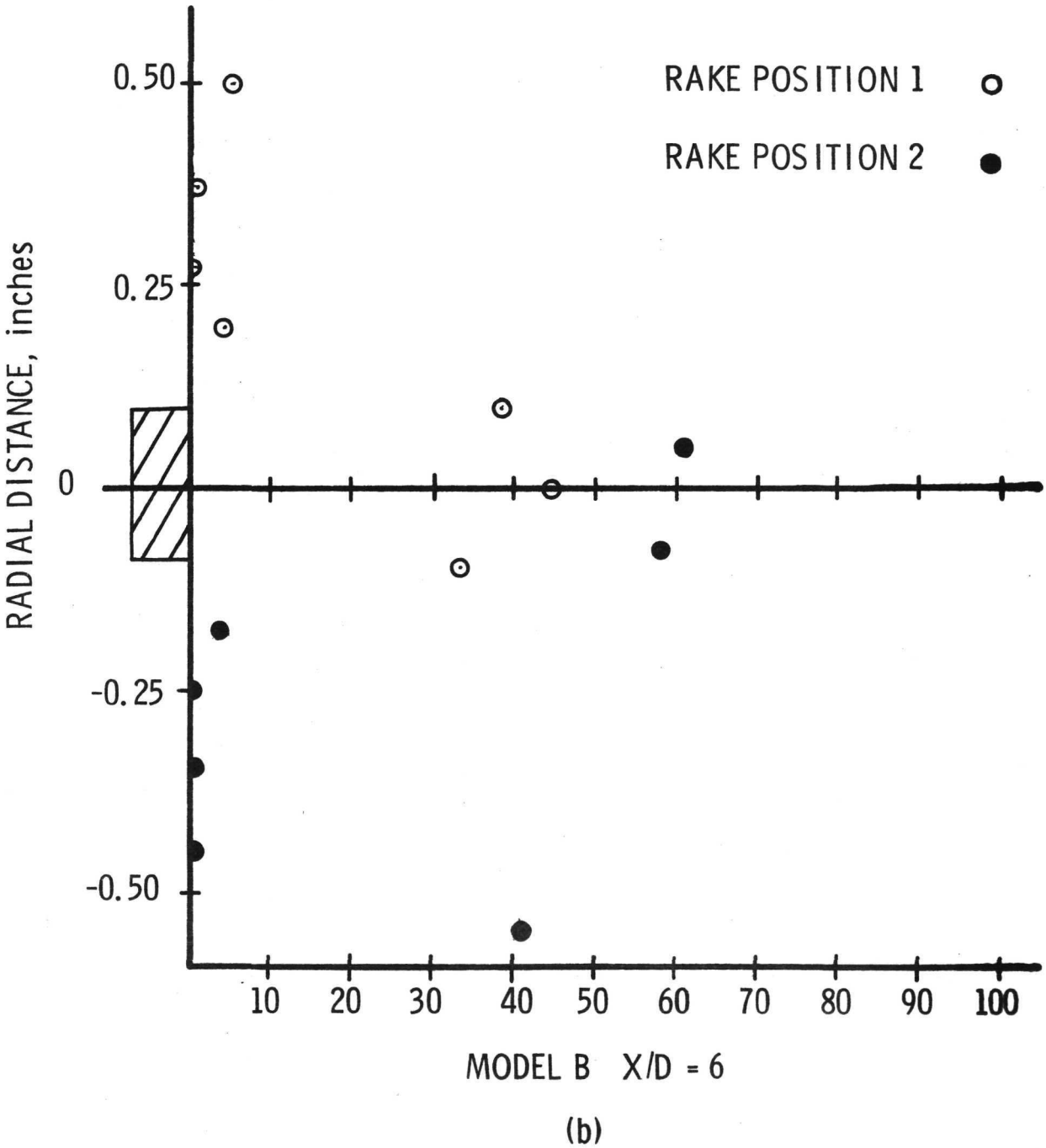
RAKE POSITION 1
RAKE POSITION 2
0.50
0.25
0
-0.25
-0.50
RADIAL DISTANCE, inches
10
20
30
40
50
60
70
80
90
100
MODEL B X/D = 6

(b)

FIG. 9 (Cont'd)

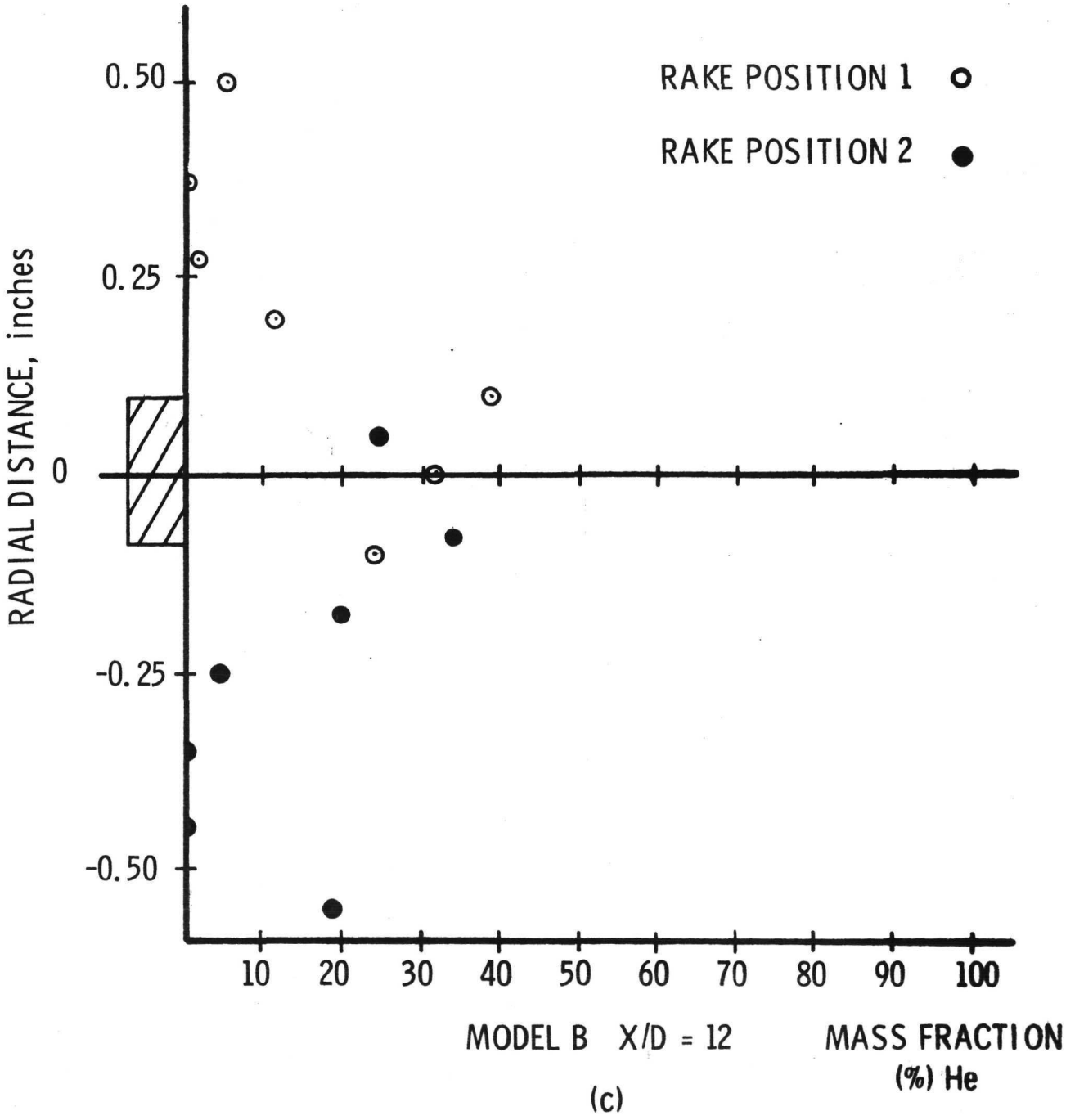
RAKE POSITION 1
RAKE POSITION 2
RADIAL DISTANCE, inches
0.50
0.25
0
-0.25
-0.50
10
20
30
40
50
60
70
80
90
100
MODEL B X/D = 12
MASS FRACTION
(%) He
(c)

FIG. 9 (Cont'd)

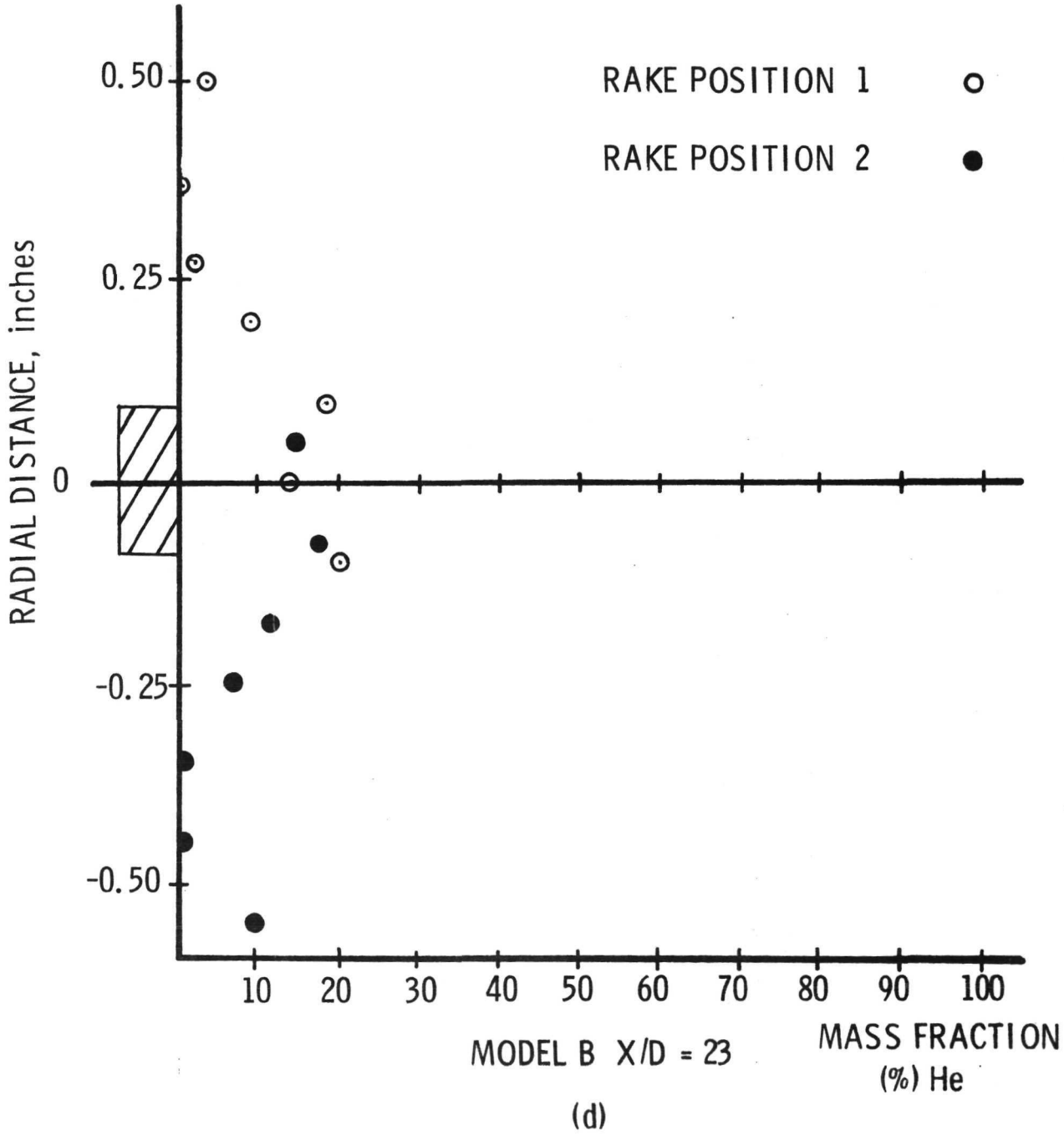
RAKE POSITION 1
RAKE POSITION 2
0.50
0.25
0
-0.25
-0.50
RADIAL DISTANCE, inches
10
20
30
40
50
60
70
80
90
100
MODEL B X/D = 23
MASS FRACTION
(%) He
(d)

FIG. 9 (Cont'd)

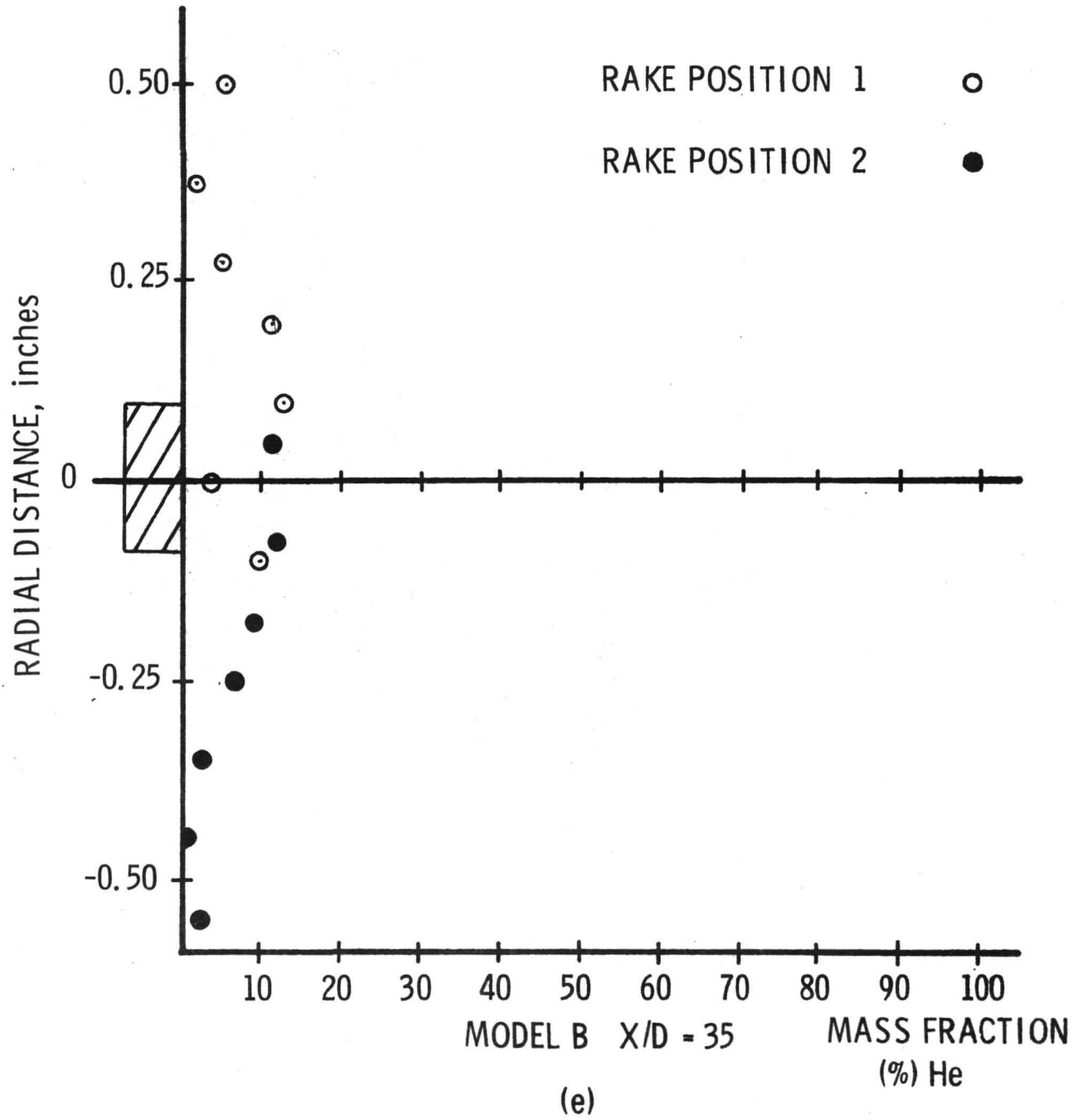
RAKE POSITION 1
RAKE POSITION 2
0.50
0.25
0
-0.25
-0.50
RADIAL DISTANCE, inches
10
20
30
40
50
60
70
80
90
100
MODEL B X/D = 35
MASS FRACTION
(%) He

(e)

FIG. 9 (Cont'd)

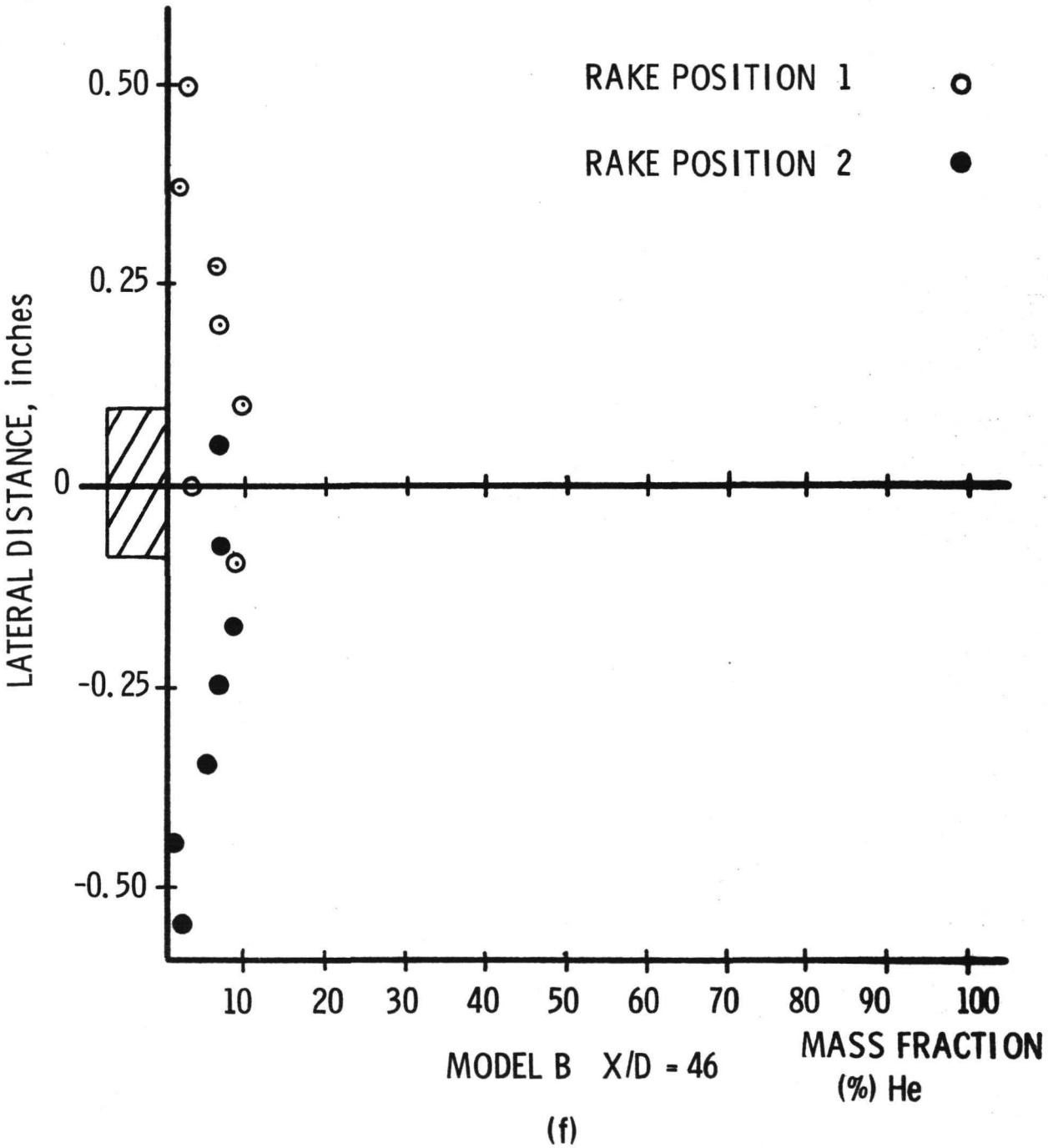
RAKE POSITION 1
RAKE POSITION 2
0.50
0.25
0
-0.25
-0.50
LATERAL DISTANCE, inches
10
20
30
40
50
60
70
80
90
100
MASS FRACTION
(%) He
MODEL B X/D = 46
(f)

FIG. 9 (Cont'd)

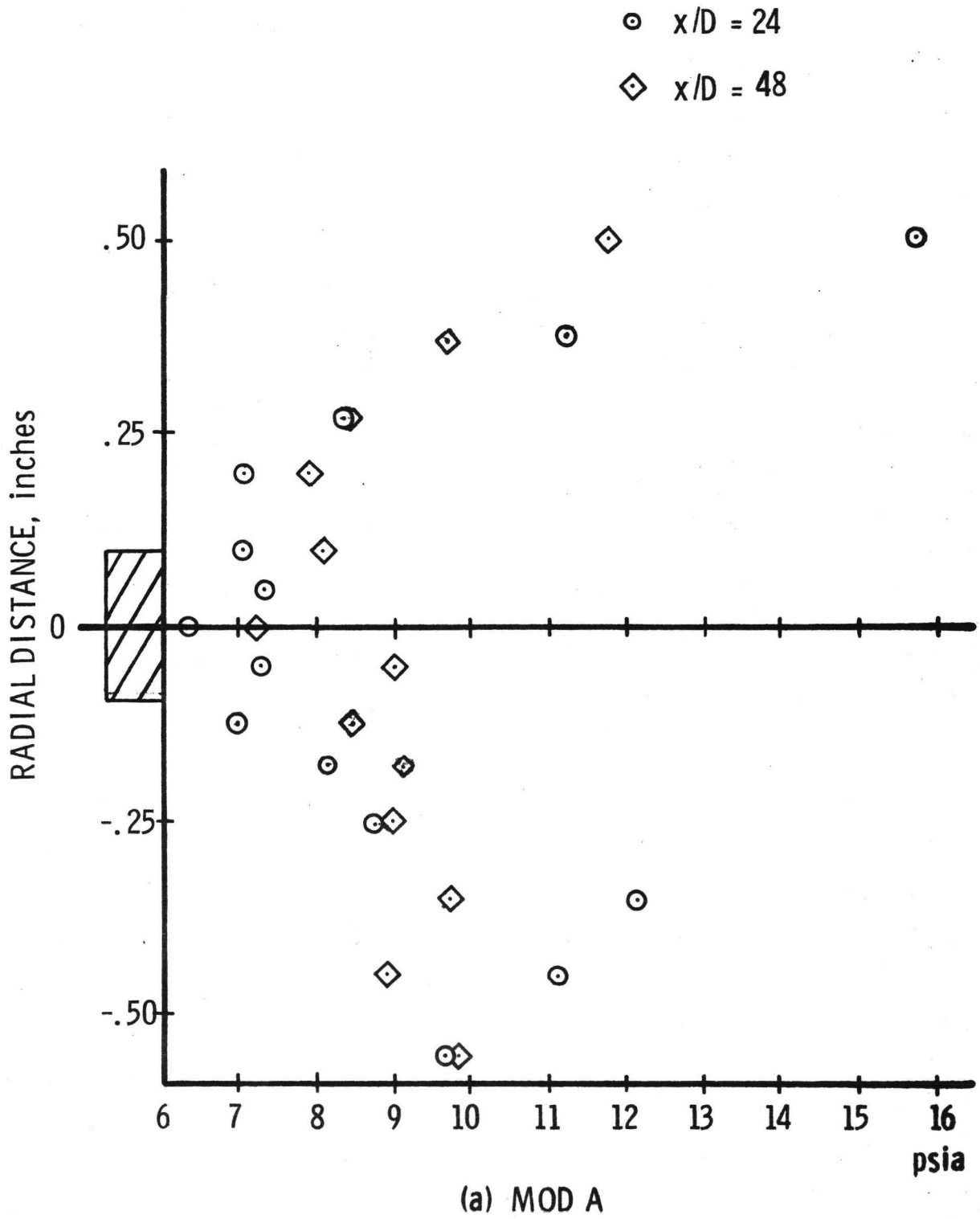

(a) MOD A

FIG. 10 PRESSURE FIELD PLOT OF TUNNEL FLOW

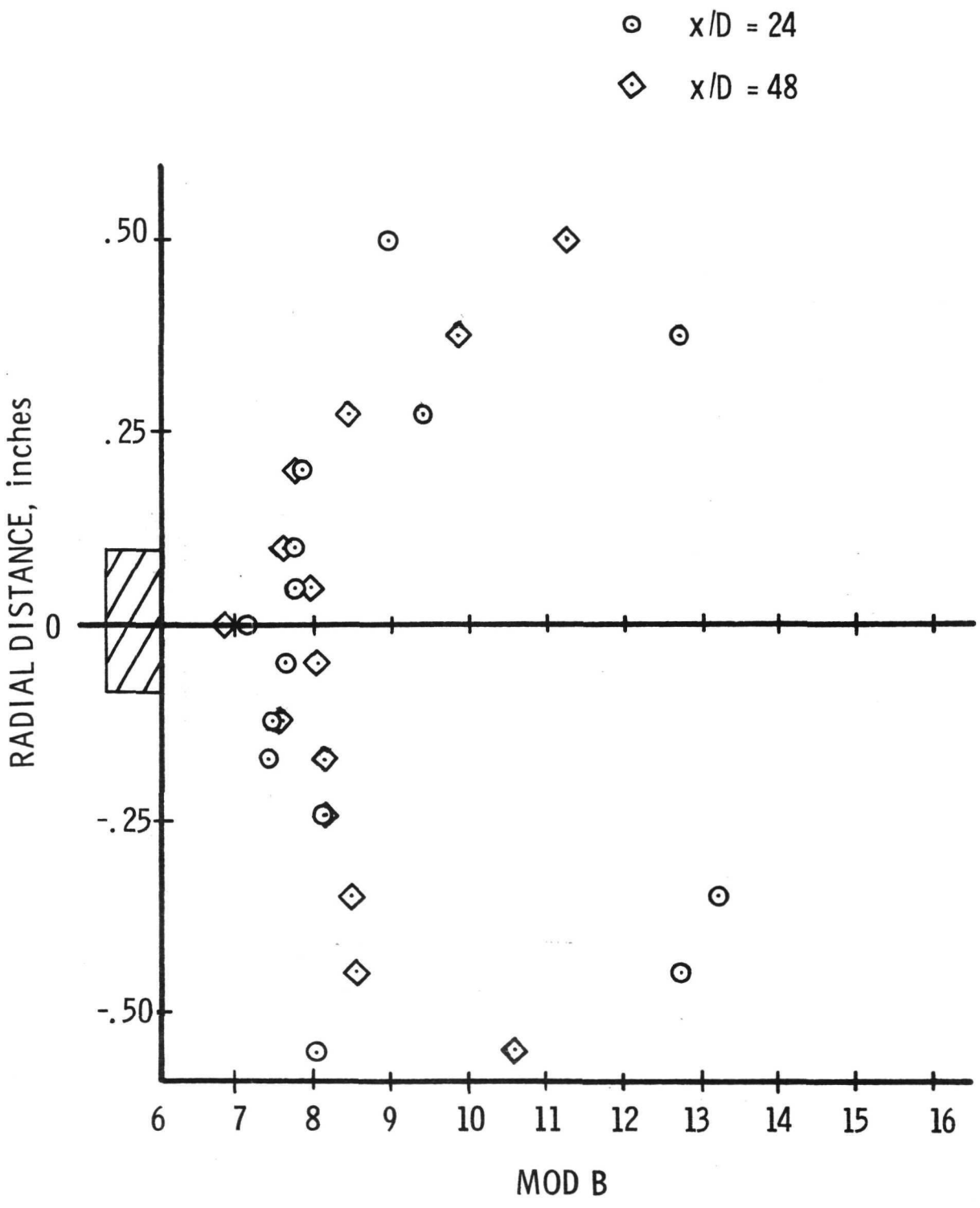
x/D = 24
x/D = 48
.50
.25
0
-.25
-.50
RADIAL DISTANCE, inches
6
7
8
9
10
11
12
13
14
15
16
MOD B

FIG. 10 (Cont'd)

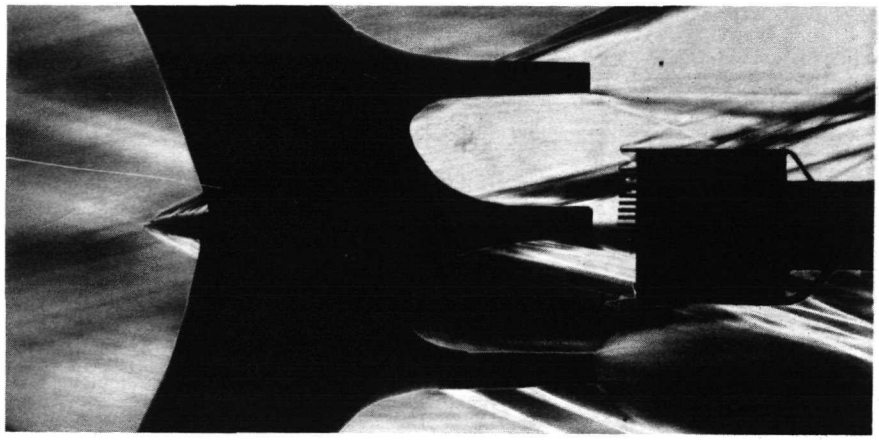

(a) Probe Position 1

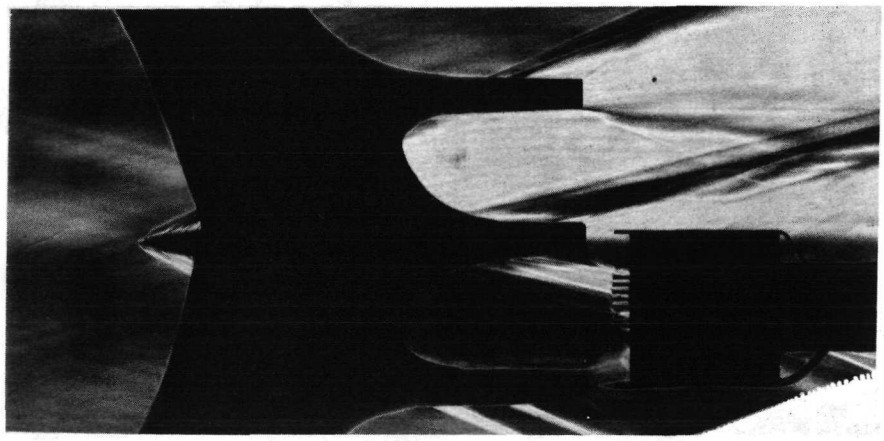

(b) Probe Position 2

Fig. 11 Schlieren Photographs Showing Probe in Measuring Positions, Mod. B.

FIG. 12 A TYPICAL GAS CHROMATOGRAPH OUTPUT TRACE

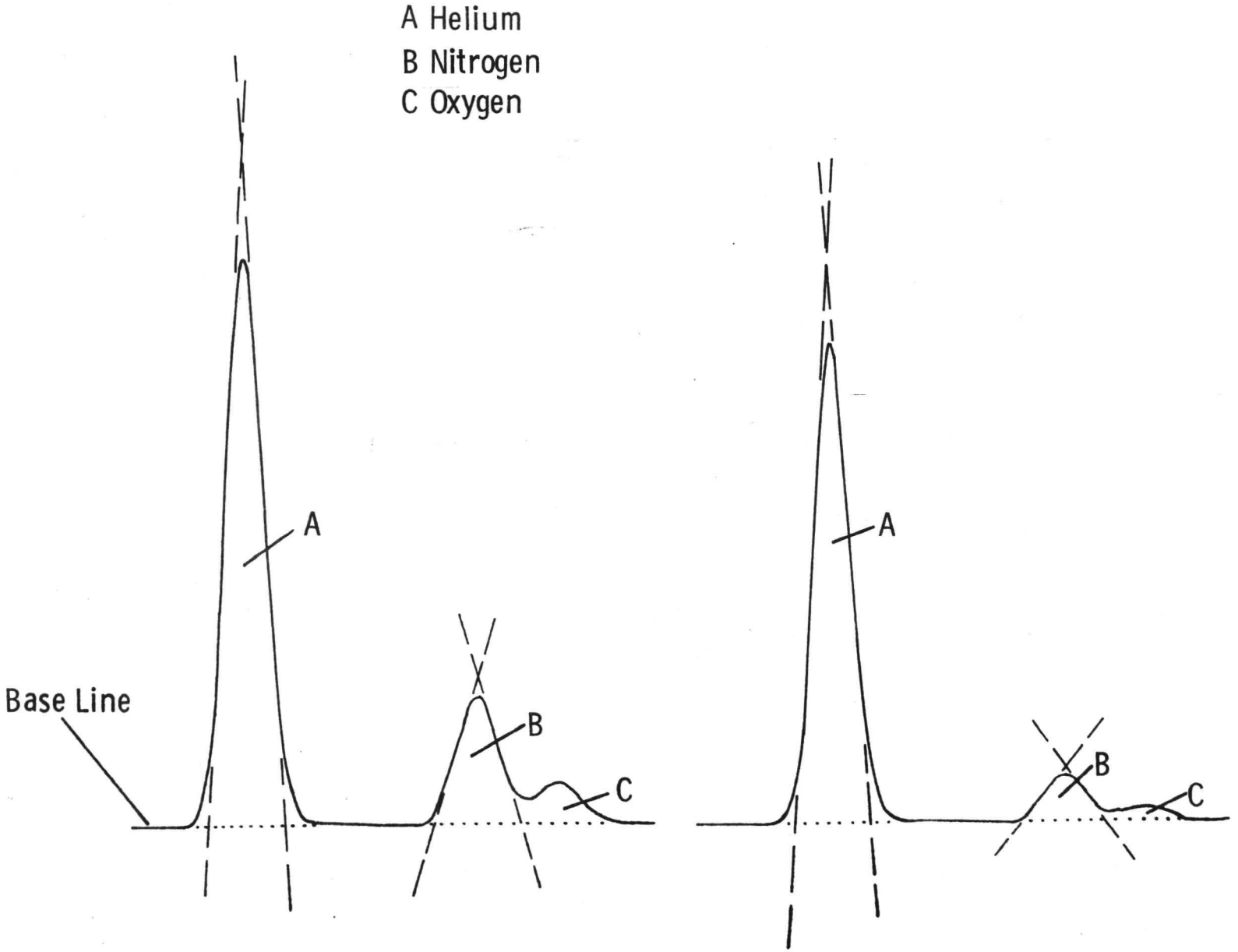

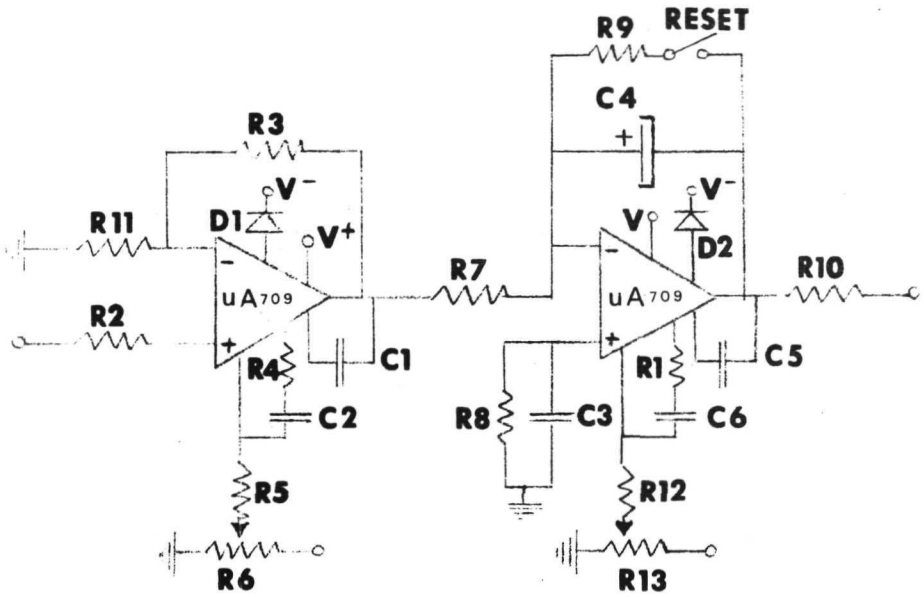

POWER SUPPLY: 15 VOLT DC

INPUT: 100 MV DC MAX. 0.5 MV DC MIN.

R_1, R_2, R_8, R_9, R_{11} = 1000 Ω

R_4 = 1500 Ω

R_3, R_6, R_7, R_{12}, R_{13} = 100 KΩ

R_{10} = 220 KΩ, R_5 = 470 KΩ

C_1, C_5 = 3 PF, C_3 = 1000 PF

C_2, C_6 = 100 PF, C_4 = 100 μF

D_1, D_2 = 1N009

OPERATIONAL AMPLIFIER μA709 DUAL INLINE

Fig. 13 INTEGRATOR CIRCUIT FOR GAS-CHROMATOGRAPH

APPENDIX A

SUPERSONIC WIND TUNNEL DESCRIPTION

APPENDIX A

9" x 9" SUPERSONIC WIND TUNNEL

The V.P.I. 9 x 9 in. supersonic wind tunnel was designed and originally constructed at the Langley Aeronautical Laboratory. In 1958 the tunnel was purchased by V.P.I. and after being re-constructed in a specially designed building was put into operation in 1963. During recent years several modifications were introduced into the air pumping, tunnel control and instrumentational equipment which increased capabilities of the facility.

The facility is of an intermittent, blow-down type with interchangeable contoured nozzles. The air pumping system consists of eight Ingersoll Rand, Model 90, reciprocating compressors, of 800 hp total capacity. They can pump the storage system up to 150 psig. A very efficient drying and filtering system is provided which includes both drying by cooling and drying by adsorption. The latter is accomplished by a fully automated system fabricated by the Kamp Co. and uses molecular sieves and activated alumina as desiccant. Air storage system consists of 16 tanks with a total volume of 2800 ft.^{3}. Tunnel control system includes a quick opening butterfly valve and a pressure regulating system.

The settling chamber contains a perforated transition cone, several damping screens and probes measuring stagnation pressure and temperature. The nozzle chamber is interchangeable with two-dimensional contoured nozzle blocks made of steel. The tunnel is equipped with three complete nozzle chambers which presently are fitted with the nozzles for the Mach numbers 2.4, 3 and 4. Several other nozzle blocks are available (not calibrated).

The working section of the tunnel is equipped with a remotely controlled model support which allows one to vary the position of a model in the vertical plane.

An arrangement for side wall model mounting is also available. An extractable mechanism can be provided for supporting the model during the starting and stopping of the flow. Due to large windows in the nozzle and working sections a very good access to the model is ensured.

After passing through a diffuser the air flow is discharged into the atmosphere outside of the building.

Technical Specification of the tunnel:

Test Section size	9 x 9 inches
Stagnation pressure	40 - 120 psia
Mach number	2.4 - 4
Reynolds number per foot	6×10^6 to 15×10^6
Run duration, depending on	
Mach number	10 - 90 sec.
Dewpoint	below -40°C
Maximum model diameter at M=3	3.5 in.
Storage tank volume	2800 $ft.^3$
Maximum air pressure in	
the storage tanks	150 psig
Total power rate of the	
compressor plant	800 hp

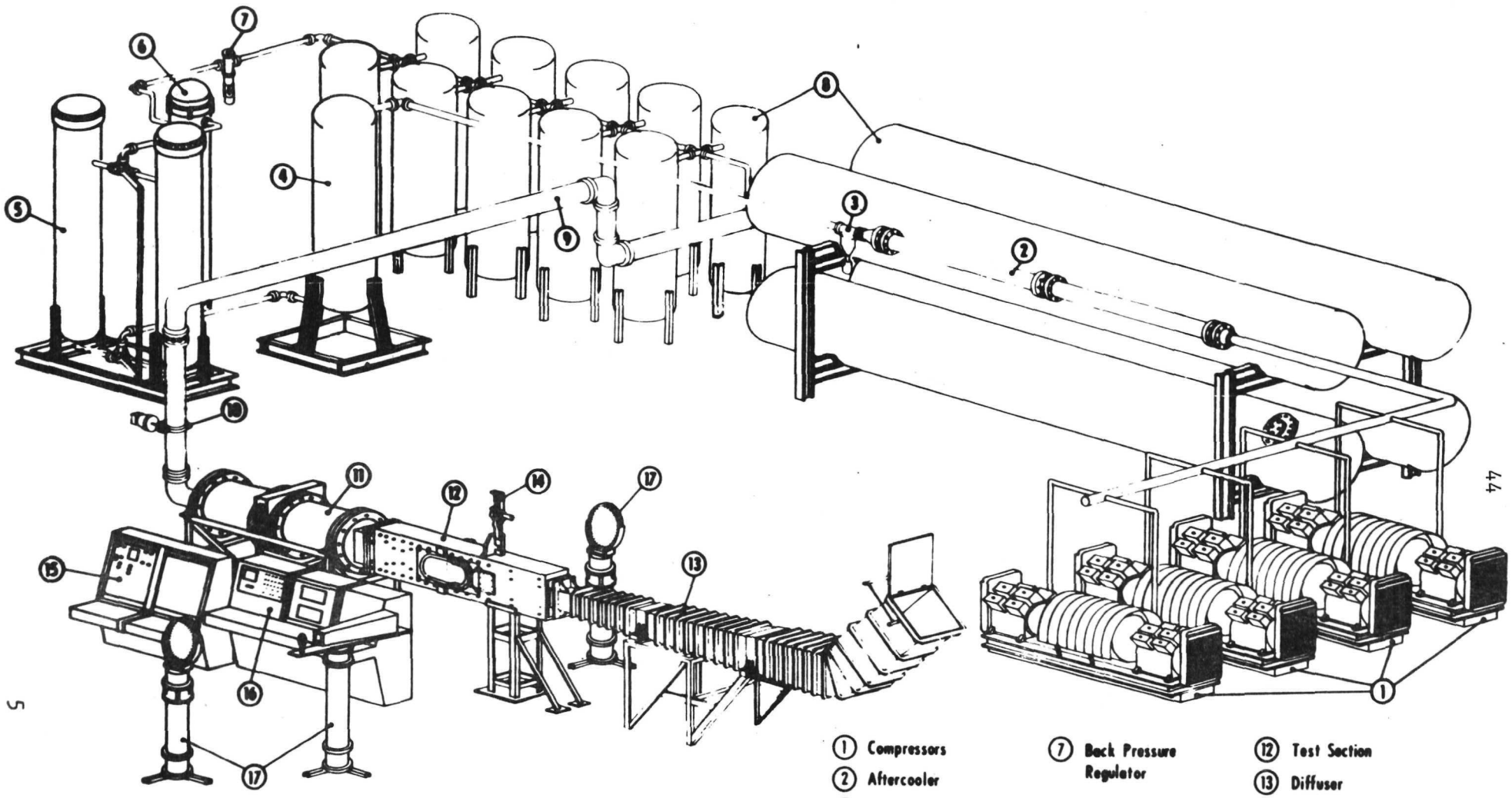

V.P.I. 9x9 in. SUPERSONIC WIND TUNNEL

1. Compressors
2. Aftercooler
3. Water and Oil Remover
4. Pre-Filter
5. Dryer
6. After Filter
7. Back Pressure Regulator
8. Storage Tanks
9. Inlet Pipe
10. Pressure Regulator
11. Settling Chamber
12. Test Section
13. Diffuser
14. Model Support and Drive System
15. Tunnel Control Panel
16. Measurement Panel
17. Schlieren Apparatus

APPENDIX B

GAS ANALYSIS METHODS

Following collection of the samples in the bottles shown in Fig. 6, the cart was moved to the analysis laboratory where the gas chromatograph was located. Here, the bottles were pressurized to a level of approximately 50 psia with argon so that the samples could be run conveniently through the chromatograph. Since argon was used as the carrier gas, the dilution of the sample by the pressurization process had no effect on the analysis. Also, all lines were purged with argon before a bottle was opened for pressurization to prevent possible contamination with air.

To insert a sample into the chromatograph for analysis, a bottle was connected and opened to permit flow through the loop of the sample valve. After allowing a sufficient flow to purge the line, the valve was rotated and the sample run through the column and cell. Columns, made by Bendix Corp. were 12' long and filled with chromosorb 102. The output was read on a Hewlett-Packard strip chart recorder with the scale set according to the estimated analysis of the sample. For example, samples with a high helium concentration sometimes required a 50 mv full-scale setting, while those which were essentially pure air produced a maximum reading of less than 1 mv. A typical trace is given in figure 12.

The actual concentrations are calculated according to following procedures[5]. The sample loop in the chromatograph is of 0.1 ml volume. Weights of 0.1 ml of pure air and He at atmospheric pressure are calculated. A pure sample of each gas is run through the gas chromatograph and the output area for He and N_2 are carefully calculated. The ratio of these areas is multiplied by ratio of actual weight of N_2 and He. This gives a factor k (corrected for air as different from N_2) which is used to multiply all N_2 readings to obtain true mass percentage as follows

$$\frac{(\text{Area He})}{(\text{Area He}) + (\text{Area } N_2) \times k} 100 = \% \text{ He in sample}$$

The factor k was recalculated regularly because of the possibility of drift in the electronic system of the gas chromatograph. The areas under the output traces can be found in one of two ways depending upon the relative concentrations of helium and air in the samples.

For samples with a helium concentration of less than approximately 60%, it is convenient to use an analog integrator circuit to give the areas directly as the sample goes through the instrument. We have developed a suitable circuit which is shown in Fig.13. The pulse duration of the helium, which comes first, is roughly 5 seconds, and the time constant of the integrator was made 10 seconds to catch the second pulse which comes approximately 3 seconds later. The output of the chromatograph is amplified approximately 100 times before integration. The amplification can be varied by changing R_3. With R_3 = 100 kΩ, the maximum output is 100 millivolts DC. The output of the integrator increases up to a maximum limit of 10 volts. To avoid noise problems, the input signal should be greater than 1 mv.

For higher helium concentrations, there is too great a disparity between the height of the helium peak and that of air for the integrator to discriminate accurately. In this region, it is most accurate and convenient to use the triangulation method[5] to determine the areas under the curves by hand. It was found necessary to switch the range of the recorder between the helium and air peaks in order to obtain reasonable accuracy in the integration calculation.

APPENDIX C

TABULATED DATA

MOD A

PITOT PRESSURE, psia

		PROBE NUMBER							
	POSITION	1	2	3	4	6	9	11	cone static pressure
x/D	1	15.77	11.22	8.37	7.05	7.03	6.38	6.97	1.13
23	2	7.3	7.27	8.13	8.77	12.13	11.15	9.67	1.13

		PROBE NUMBER							
	POSITION	1	2	3	4	6	9	11	cone static pressure
x/D	1	11.8	9.75	8.47	7.93	8.10	7.3	8.47	1.13
46	2	---	9.07	9.13	9	9.76	8.93	9.82	1.28

MOD B

PITOT PRESSURE, psia

	POSITION	PROBE NUMBER 1	2	3	4	6	9	11	cone static pressure
x/D	1	8.96	12.76	9.44	7.87	7.79	7.14	7.46	0.96
23	2	7.79	7.62	7.46	8.12	13.29	12.79	8.02	1.29

	POSITION	PROBE NUMBER 1	2	3	4	6	9	11	cone static pressure
x/D	1	11.29	9.89	8.42	7.79	7.62	6.87	7.59	0.973
46	2	7.96	8.02	8.13	8.13	8.49	8.52	10.61	1.39

MOD A

% H_e By Mass

		x/D					
	SAMPLE NO.	1	6	12	23	35	46
Position 1	1	1.6	0	0.1	0.3	0.8	1.2
	2	5.2	1.5	0.18	2.5	2.5	2.6
	3	0.6	0.3	4.5	7.9	7	6
	4	0.25	14	15.5	17.6	11.8	---
	5	85	62	55	35.5	18	11.4
	6	36	22	21.5	13	12	7.6
	7	55	6.5	10	13.9	11.5	7.6
Position 2	1	53.5	50	38.5	13.6	14	6.6
	2	100	20.5	12	11.1	11.4	9.5
	3	0	4.5	12	8.6	8.5	6.6
	4	0	0	4.2	6.5	7.5	6.0
	5	0.1	0	0	1.2	3.7	3.7
	6	0	0	0	0.1	1.3	3.2
	7	0	0	0	0.4	2.0	4.5
Position 3	1	3	0	0	0.3	---	---
	2	0.5	4	0.4	0.8	---	---
	3	0.2	0.2	11.5	3.8	---	---
	4	0.3	0.4	49.5	21.7	---	---
	5	0.2	60	52	3.2	---	---
	6	38.5	53	28.5	5.1	---	---
	7	62	85	14.5	0.36	---	---

Position 1 refers to upper position of rake; (Rake probe No. 9 is centered on the flow). Position 2 is 0.45" lower than 1 and Position 3 another 0.45" lower.

MOD B

% H_e By Mass

		x/D					
	SAMPLE NO.	1	6	12	23	35	45
Position 1	1	0	5.6	5.2	3.5	5.5	2.5
	2	0	1.0	0.7	0.4	2.0	1.8
	3	0	0	2.0	2.2	5.0	6.0
	4	0	4.2	11.5	8.9	11.0	6.5
	5	14	38.5	38.5	18.2	12.5	9.5
	6	56	45	31.5	14	3.0	3.0
	7	71	33.5	24	20	9.5	8.5
Position 2	1	64	61	24.5	14.5	1.5	6.3
	2	54	58	34	17.5	12.0	6.6
	3	15.5	4	20	11.5	9.0	8.0
	4	0	0.25	4.5	6.5	6.5	6.5
	5	0.1	0	0	0.8	2.8	5.0
	6	0.1	0.7	0	0.8	0.5	1.0
	7	0.2	41	18.5	9.5	2.5	2.0